Sensitivity of iceberg drift and deterioration simulations to input data from different ocean, sea ice and atmosphere models in the Barents Sea~~(Part II)~~.

Lia Herrmannsdörfer[1], Raed Khalil Lubbad[1], and Knut Vilhelm Høyland[1]

[1]Norwegian University of Science and Technology, Trondheim, Norway

Correspondence: Lia Herrmannsdörfer (lia.f.herrmannsdorfer@ntnu.no)

Abstract. Iceberg ~~data~~ observations in the Barents Sea ~~is~~ are scarce. Numerical simulations of iceberg drift and deterioration ~~as function of the environmental conditions, e.g. from models of atmosphere, ocean and sea ice, provide a useful mean to bridge~~ help fill this gap. The ~~simulation results rely on the quality of the input data . We~~ quality of these simulation results depends, among other factors, on the accuracy of the environmental data (e.g., wind, waves, currents, salinity, temperature), often derived from ocean, sea ice and atmosphere models. In this study, we conduct a numerical experiment ~~, in which we force an iceberg~~ simulating the drift and deterioration ~~model with combinations of~~ of a large number of synthetic icebergs. We force the iceberg model with two atmospheric reanalyses (ERA5, CARRA) and two ocean and sea ice models (Topaz, Barents-2.5) in the Barents Sea ~~and the years of~~ for the years 2010-2014 and 2020-2021. ~~Further, the impact on the simulation results is analysed. We found~~ The differences in iceberg model output are statistically quantified, illustrated using an exemplary trajectory, and explained based on variations in environmental input. We conclude that simulation results of iceberg drift and deterioration are highly sensitive to the choice of the ~~ocean and sea ice forcing data. The horizontal resolution bathymetry of the forcing data, especially in proximity to the coastlines, influence the availability and representability of the forcing information and, thus, the iceberg simulation results (e.g. occurrence and extent). Deviations in the ocean and sea ice variables~~ environmental input, depending on the simulation goal, time frame, area of interest and input characteristics. Iceberg simulations using input from Barents-2.5 yielded a distinct regional distribution of iceberg density, $8\,\mathrm{days}$ longer drift duration, and $-6.2 \cdot 10^4\,\mathrm{kg}$ lower deterioration trend. These differences are primarily attributed to lower sea surface temperature ($-0.41\,^{\circ}\mathrm{C}$), higher ice concentration (4%), larger exposure to sea ice (23%), larger water speeds ($0.05\,\mathrm{ms}^{-1}$) and the representation of tides and topographically-steered currents in Barents-2.5~~and Topazcaused considerable differences in the simulated large-scale and regional iceberg occurrence in the domain. The impact is especially large for sea ice variables. The impact of varied atmospheric forcing is secondary. In spite of varied environmental forcing, surprising similarities in the main iceberg pathways were observed.~~ , compared to Topaz. Atmospheric input has little impact on most iceberg characteristics. The iceberg pathways and their southern extent remain largely insensitive to variations in environmental input.

1 Introduction

The Barents Sea is subject to icebergs calved from the tidewater glaciers of Svalbard, Franz-Josef-Land and Novaya Zemlya (Abramov and Tunik, 1996). The number of iceberg observations is limited due to their ~~comparably small size,~~ rare occurrence in the more ~~inhabited~~ navigated southwestern Barents Sea and the general sparseness of observations in the Arctic. In contrast to to Greenlandic icebergs, these icebergs are small compared to typical satellite resolutions available for observing icebergs. Statistics of iceberg occurrence therefore rely heavily on numerical simulations.

Such simulations describe the interaction of ~~ice features~~ icebergs with the atmosphere, ocean and sea ice. Iceberg drift is steered by the sea water motion, waves, wind, sea ice drift, sea surface slope~~and coriolis forces~~ , coriolis forces and interaction with the sea floor (Savage, 2001). Icebergs deteriorate by wave erosion, calving, forced convection ~~by~~ due to the differential velocities of iceberg, sea water and wind, buoyant vertical convection and solar radiation (El-Tahan et al., 1987; Savage, 2001). Previous studies (Kubat et al. (2005, 2007); Eik (2009b, a); Keghouche et al. (2009, 2010)) investigated the relative importance of those parameters and validated their model implementations with ~~observational and~~ exemplary observational or experimental data. Other studies (Monteban et al. (2020); Keghouche et al. (2010)) used such iceberg models to produce long-term statistics of iceberg occurrence. Eik (2009b) highlighted the influence of the environmental ~~forcing~~ input and concluded that a large part of the uncertainties ~~resolves~~ results from the environmental input, e.g. from ocean reanalyses.

~~Due to its diverse bathymetry and position between warm Atlantic waters and the cold Arctic Ocean, the Barents Sea exhibits highly complex interaction of ocean and atmosphere. Those interactions are described in atmospheric, ocean and sea ice models, with different resolution and physical description.~~

This paper is dedicated to study the impact of varied ocean, sea ice and atmosphere ~~forcing~~ input on simulations of iceberg drift and deterioration in the Barents Sea. The results ~~shall~~ aim to support the selection of environmental input for iceberg simulations to improve the accuracy of iceberg predictions and statistics in the Barents Sea~~and shall also support the choice of environmental forcing for iceberg simulations~~ . More accurate iceberg simulations will increase the safety of human operations in icy waters.

Therefore, a stat-of-the-art model for the simulation of iceberg drift and deterioration in the Barents Sea described by Monteban et al. (2020) is used herein to perform a numerical experiment. In the experiment, the iceberg model is forced by ~~various combinations of~~ combinations of state-of-the-art ocean and atmosphere reanalyses, hindcasts and forecast systems, ~~of different resolution and representativity of the domain,~~ namely *Arctic Ocean Physics Reanalysis (Topaz)* ~~(?)~~(Xie, J., et al., 2017), the Barents-2.5 forecast system ~~(?)~~(MET-Norway, a), the Barents-2.5 hindcast (MET-Norway, c), the *global atmospheric reanalysis ERA5* (Hersbach et al., 2023) and the *Arctic regional reanalysis CARRA* (Schyberg et al.). These environmental models describe the highly complex interaction of ocean and atmosphere of the Barents Sea due to its complex bathymetry and position between warm Atlantic waters and the cold Arctic Ocean with different resolution, model physics and representativity of the

domain. While those differences have been characterised for ERA5 and CARRA (e.g. in Køltzow et al. (2022)), the literature lacks a systematic comparison of Topaz and Barents-2.5. We statistically quantify the differences between the environmental models for the Barents Sea over the years 2010-2014 and 2020-2021. This detailed and case-specific knowledge is related to model descriptions and quality information from literature. This novel composite of knowledge about the differences in ocean, sea ice and atmosphere variables is used in the core of this study to examine the effects of these differences on iceberg drift and deterioration simulations in the Barents Sea.

~~A total of 72884 icebergs $(4 \cdot 2603 \cdot 7)$is simulated and the results are analysed statistically (Sect. **??**-4.3). Further we examined one exceptional iceberg trajectory (Sect.4.4). The differently-forced simulations are compared regarding~~

The iceberg drift and deterioration simulations are performed for a large number of simulated synthetic icebergs in the Barents Sea. The simulation results with varied environmental input are compared statistically with respect to various characteristics of the simulated iceberg trajectories, i.e. ~~the availability of forcing data in the iceberg model's data assimilation (Sect. **??**), iceberg deterioration(Sect. **??**)~~iceberg deterioration, iceberg drift (**??**4.1) and resulting distribution in the domain (Sect. 4.2, 4.3).

Further, we examine one synthetic iceberg trajectory to illustrate the statistical results (Sect. 4.4). In the discussion (Sect. 5), the differences ~~of~~ between the simulations with varied ~~forcing~~ environmental input are traced back to the differences ~~of the forcing variables and their origin in the setup of the~~ between the ocean, sea ice and atmosphere models, ~~described in the preceding study , **?**~~that we quantify in Sect. 3. We further discuss the suitability of the environmental datasets in different applications of iceberg simulations (Sect. 5.1).

We emphasise that this study focuses on the impact of the choice of environmental input data on iceberg statistics rather than analysing on the absolute iceberg statistics. We refrain from analysing the impact of iceberg model settings on iceberg statistics and inherit the iceberg model settings from Monteban et al. (2020). We do not compare to observations of iceberg trajectories, as we choose a purely statistic approach and observations are scarce.

2 Description of the Experiment

A numerical experiment is conducted in which ~~the model of Monteban et al. (2020) for~~ an iceberg drift and deterioration model (Monteban et al., 2020) is forced by different combinations of ocean, sea ice and atmosphere ~~data sets to determine~~ datasets assess the impact of ~~varied forcing~~varying environmental input. This Section provides an overview ~~on the experiment , input data~~ of the experiment and the iceberg model. A detailed description of the iceberg seeding, ~~the iceberg~~ model setup, ~~the~~ drift and deterioration equations, ~~the equation parametersand the computational routines are given~~ parameters, and computational routines is provided in the Appendix (Sect. A).

2.1 Experiment setup

The iceberg model is forced by ~~the~~ four combinations of the ocean, sea ice and atmosphere data~~shown in Table ??. The forcing combinations represent a reference case with global forcing (~~. The combinations are i) the reference case using the global models Topaz and ERA5 ~~) and a~~ (12.4 km and 31 km horizontal resolution), ii) the high-resolution, regional simulation ~~(with~~ case using Barents-2.5 and CARRA (both 2.5 km). The ~~other combinations~~ combinations Topaz and CARRA (12.4 km and 2.5 km) and Barents-2.5 and ERA5 (2.5 km and 31 km) serve to estimate the individual influence of ocean, sea ice and atmosphere ~~forcing~~ input on the simulations results. We did not conduct a full sensitivity analysis~~for every variable , as this would cause physical inconsistency and does not reflect~~ , varying every variable individually, to avoid physically inconsistent input (of e.g. SST and CI) and to resemble a probable use case as closely as possible. The simulations are performed for the years 2010-2014 and 2020-2021~~(), due to limitations in the data availability~~ , which were the only years all environmental datasets were available at the time the simulations were performed. ~~Following, a total number of 2603 · 7 icebergs are simulated in four different forcing combinations.~~

~~Combinations of environmental forcing from ocean, sea ice and atmospheric reanalyses, hindcasts and forecasts in the numerical experiment. Objective Ocean & sea ice Forcing Atmospheric Forcing Reference, global Topaz ERA5 Regional wind Topaz CARRARegional ocean & sea ice Barents-2.5 ERA5 High resolution, fully regionalBarents-2.5 CARRA~~

2.2 ~~Data~~

~~This Section provides an overview on used variables, data sources and applied pre-processing. A detailed description is given in ?.~~

~~We use 10m wind ($\boldsymbol{v}_{\mathrm{a}}$) from Global Atmospheric Reanalysis ERA5 (Hersbach et al., 2023) and Copernicus Arctic Regional ReAnalysis CARRA (Schyberg et al.). The sea surface velocity ($\boldsymbol{v}_{\mathrm{w}}$) and surface temperature (SST), as well as, the sea ice concentration (CI), thickness (h_{si}) and drift velocity ($\boldsymbol{v}_{\mathrm{si}}$) are obtained from the Arctic Ocean Physics reanalysis based on Topaz4b (?) (Topaz), Barents-2.5 forecast (2020-2022) (?) and Barents-2.5 Hindcast (2010-2014) (MET-Norway, c). Further, geostrophic currents are gathered from Slagstad et al. (1990) and bathymetry is gathered from (Jakobsson et al., 2012).~~

~~To reduce memory requirements, a spatial subset of the Barents Sea is applied. Note, that the subsets differ for the forcing data sets, due to their varying grid type, resolution and orientation. The ERA5 and CARRA data is masked for grid cells with at least ocean content, based on their native land-sea-masks~~Despite the small number of years included and large interannual variability, we characterise the two most recent decades with sea ice regimes at different stages of the advancing climate change. Future studies may concern themselves with analysing the newly available, extended time period.

~~For an efficient simulation process, velocity variables are translated to components in the longitudinal (u) and latitudinal (v) direction. In addition, temporal data gaps on the scale of hours to few days are replaced by the previous or following time step for a more consistent forcing in the iceberg simulations.~~

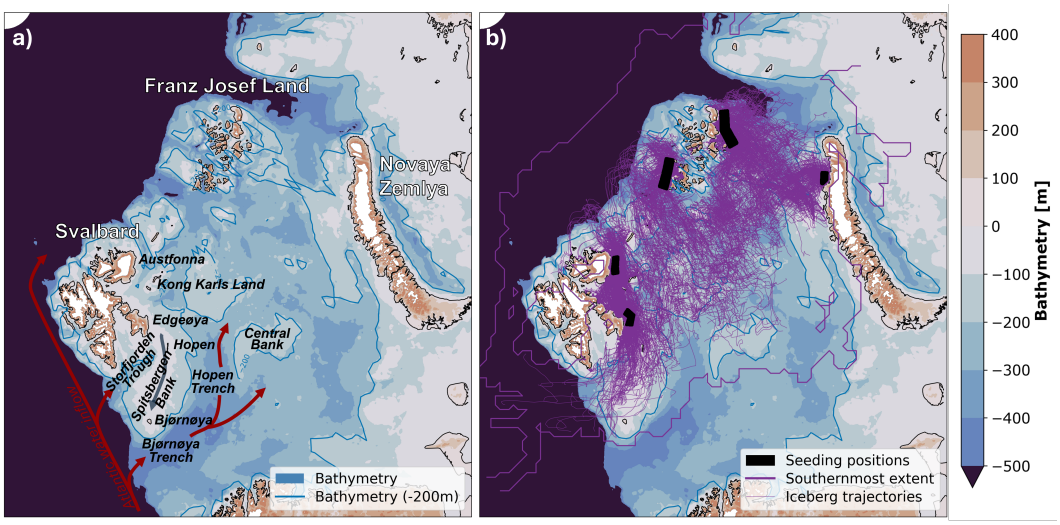

Figure 1. Map of the Barents Sea (a) and main simulated iceberg pathways (b) with seeding regions (black areas), the maximum simulated iceberg extent (thick purple lines) and an exemplary subset of the trajectories (thin purple lines).

2.2 Iceberg seeding

Icebergs are seeded ~~at a random position close to~~ near the tidewater glaciers of Franz-Josef-Land, Austfonna, Edgeøya and Novaya Zemlya ~~and a random day from 1 July to 30~~ (Fig. 1) from July to November of the ~~simulations~~ years 2010-2014 and 2020-2021. The iceberg length is ~~drawn randomly~~ sampled from a generalised extreme value (GEV) distribution~~, derived from satellite observations at each of the sources by Monteban et al. (2020). The iceberg width and height are derived by empirical relations. The~~ . The minimum initial iceberg length is ~~defined by~~ set at $34\,\mathrm{m}$, corresponding to the maximum resolution of the satellite observations and the definition of a bergy bit ($10\,\mathrm{m}$ height). ~~This initial conditions~~The iceberg width and height are derived from empirical relations described by Dezecot and Eik (2015). The set of seeded icebergs is representative of the domain, as the size and number of seeded icebergs are based on satellite observations near the glaciers (Monteban et al., 2020) . A meaningful statistic is ensured by a randomised seeding day, location and length within this observed range, thus exposing them to a random selection of environmental conditions. These initial settings vary for all ~~2603 icebergs released within one simulation year and the 7 simulation years, but is reproduced in the~~ released icebergs but are identical for simulations with varied ~~forcing~~environmental input. More details on the seeding approach are given in the Appendix (Sect. A). Note that the seeding locations are far enough to the coastline to avoid grounding during the initial phase of the simulations.

2.3 Model for iceberg drift and deterioration

The numerical model for the simulation of iceberg drift and deterioration is ~~adapted from Monteban et al. (2020) to suite the requirements of this study. The~~ inherited from Monteban et al. (2020) with its model settings. The iceberg model is Lagrangian and deterministic. The iceberg drift is simulated based on wind, sea water velocity, sea ice drift~~and the resulting~~

~~coriolis force~~ , the resulting Coriolis force and interaction with the sea floor. The pressure gradient forces are approximated with the geostrophic currents~~from Slagstad et al. (1990). Wave drag~~ . Wave forces are included ~~in~~ by calibrating the wind drag coefficient implicitly. ~~The added mass coefficient is set~~ We set added mass to zero. The iceberg melt is a function of basal turbulent melt, vertical thermal buoyant convective melt and wave erosion based on wind, water velocity and the sea surface temperature. The iceberg drift categorises "light" sea ice ($CI > 15\%$) and "heavy" sea ice ($CI \geq 90\%$ and $h_{\mathrm{si}} \geq h_{\mathrm{min}} = \frac{13000}{20000 \cdot exp(-20(1-CI))}$) and neglects sea ice outside the sea ice edge ($CI \leq 15\%$). The wave erosion term does not consider swell waves as the sea state is defined only by wind and water velocity. Melt by solar radiation is neglected due to its minor influence in the far north and calving is not explicitly ~~described~~modelled. The drift and deterioration equations and model parameters are given in the Appendix (Sect. A).

The iceberg model solves the drift and deterioration equations ~~for~~ at $2-\mathrm{hourly}$ time steps and updates iceberg position, size and velocity. The simulation is stopped when the iceberg ~~is~~ has melted to the size of a growler ($H \leq 10\,\mathrm{m}$), leaves the simulation domain or ~~time period .~~ when the desired simulation period is exceeded.

2.4 ~~Assimilation of environmental data~~

~~Environmental data is assimilated at simulation time steps at the iceberg position. Dependent on the temporal resolution of the data , forcing fields are read directly at the time steps (ERA5, Barents-2.5) or the last available time steps (Topaz, CARRA). Spatially, forcing variables are read from~~ The iceberg model assimilates environmental data from the present or most recent time step and the nearest grid cell of the respective ~~data set (*nearest forcing cell*) without interpolation, as shown in Fig. **??** (green circles). The distance is determined between the iceberg and the grid cellcentre (Fig. **??**, green lines). Note, that the environmental data sets~~ environmental dataset without interpolation. When no data is available in the nearest grid cell, we also consider surrounding grid cells at larger distance to the iceberg for better coverage of coastal regions. As the environmental datasets have different grids ~~, so that the forcing data for one time step is not raised~~ and resolutions, the input data is not necessarily assimilated from the same ~~area.~~ geographical area for the same iceberg position. In spite of the availability of more sophisticated model equations and assimilation methods, the described iceberg model exhibited its robustness in Monteban et al. (2020) and is herein used without further evaluation of the model settings' impact on the simulation results.

3 Analysis of ocean, sea ice and atmosphere data in the iceberg pathways

This study uses 10m wind ($\boldsymbol{v}_{\mathrm{a}}$) from ERA5 (Hersbach et al., 2023) and CARRA (Schyberg et al.). The sea surface velocity ($\boldsymbol{v}_{\mathrm{w}}$), sea surface temperature (SST), sea ice concentration (CI), ice thickness (h_{si}), and ice drift velocity ($\boldsymbol{v}_{\mathrm{si}}$) are obtained from Topaz (Xie, J., et al., 2017) and Barents-2.5 (hindcast 2010-2014, forecast 2020-2021) (MET-Norway, a, c). Table 1 provides an overview of the environmental models. Additionally, we use geostrophic currents from Slagstad et al. (1990) and the IBCAO 3.0 bathymetry (Jakobsson et al., 2012). All data is used at its original spatial resolution. In this study, we introduce

the term *iceberg pathways* to refer to all regions and time periods in which icebergs were simulated. Figure 1 depicts the spatial occurrence of icebergs in the Barents Sea. We analyse environmental data in the pathways, specifically environmental model grid cells and model time steps that contributed to the iceberg simulations. Figure 2 compares the environmental variables in the iceberg pathways in Fig. 2 and Tab. 2 and relates the differences to known model uncertainties.

~~Because of the gridded nature of the forcing data and the respective resolution, ocean forcing is often not available close to the coastlines. As the iceberg model is Lagrangian, has a high-resolution bathymetry and a different representation of the coastline, icebergs may drift close to (or beyond) the coastline of the forcing data set. Figure **??** illustrates an iceberg trajectory, in which the iceberg determines a land cell as nearest forcing cell, in which ocean and sea ice variables are unavailable (Fig. **??**, time step 10) . In the current implementation of the iceberg model, missing forcing along the coastlines is approximated by averaging surrounding grid cells ("neighbour average", Fig. **??**, pink squares). If the surrounding grid cells of the nearest neighbour forcing cell do not contain any data either, the search radius (Fig. **??**, purple circle) is increased step-wise, and up to a radius of 3 (for low-resolution input)or 16 grid cells (for high-resolution input)~~

Sea surface temperature

We compare the SST in Topaz and Barents-2.5 and ~~CARRA. The maximum search radius in kilometres $sr_{max}(km)$ is calculated by~~

$$sr_{\max}(\mathrm{km}) = \sqrt{2 \cdot (d \cdot sr)^2}$$

~~with the horizontal grid resolution d (e.g. for~~ find that it is 0.41°C lower for the iceberg pathways in Barents-2.5~~) and the search radius (sr)as number of grid cells (e.g. 1). In contrast, the nearest forcing cell exhibits a maximum search radius of $\sqrt{2 \cdot (d/2)^2} = \sqrt{2 * (12.4/2)^2} = 8.8\,\mathrm{km}$ for Topaz, for~~ . The spatial differences follow the bathymetry and sea ice characteristics (Tab. 2, Fig. 2). The largest differences can be seen along the inflow of warm Atlantic waters into the West Spitsbergen Current and the Barents Sea (e.g. into the Storfjorden Trough, Bjørnøya Trough and Hopen Trench), and along the spring sea ice edge. In the literature, Topaz is known to have a large positive SST bias in those regions due to issues with simulating the circulation of Atlantic water inflow and the topographic steering (Xie et al., 2017). Barents-2.5 ~~and CARRA. Note that~~ is known to have a negative SST bias and large SST mismatches in the marginal ice zone (Röhrs et al., 2023) due to two-way coupling between the model ocean and sea ice component. Topaz is described as closer to the observations than the Barents-2.5 hindcast (Idžanović et al., 2024). Note that Figure 2 presents the difference in sea ice variables between Topaz and Barents-2.5, calculated as $CI(Topaz) - CI(Barents2.5)$ within the maximum observed sea ice extent, including areas where sea ice is present only in Barents-2.5.

4 ~~Analysis~~

3.1 ~~Availability of environmental forcing data in the data assimilation~~

Table 1. Overview of ocean, sea ice and atmosphere models.

Model	Arctic Ocean Physics Reanalysis (Topaz)	Barents-2.5 Hindcast & Forecast	Global atmospheric reanalysis (ERA5)	Copernicus Arctic Regional ReAnalysis (CARRA)
What	Ocean and sea ice	Ocean and sea ice	Atmosphere	Atmosphere
Type	Reanalysis	Hindcast, Forecast (EPS)	Reanalysis	Reanalysis
Horizontal resolution	12.3 km	2.5 km	31 km	2.5 km
Temporal resolution	daily to monthly	hourly	hourly	3 – hourly
Domain	Arctic Ocean north of $50° N$	Barents Sea	Global	Barents Sea, Greenland
Time	1991-2022	2010-2022, ~~for every variable separately. If no forcing data is available within this radius, the respective forcing variable is set to zero. This corresponds to a maximum search radius of roughly grid cells for Topaz and for~~ 2020-2021 (non-EPS), 2022-present (EPS)	1950-present	1990-present
Supplier	Copernicus Marine	MET Norway	C3S	C3S
Reference	Xie, J., et al. (2017)	MET-Norway (c, a, b)	Hersbach et al. (2023)	Schyberg et al.
Literature	Sakov et al. (2012)	Röhrs et al. (2023), Fritzner et al. (2019)	Hersbach et al. (2020)	e.g. Køltzow et al. (2019)
Product used	daily surface product	Best estimate of shortest lead time 2010-2014 hindcast and 2020-2021 (non-EPS) forecast	Analysis on single levels	Analysis on single levels (Eastern domain)

Table 2. Statistics of ocean, sea ice and atmosphere variables in Topaz and Barents-2.5, ERA5 and CARRA for the simulated iceberg pathways in the Barents Sea (spatial grid cells and time steps used in the iceberg simulations). The variables are sea surface temperature (SST), sea surface speed (v_w), sea ice concentration (CI), sea ice thickness (h_{si}), sea ice drift speed (v_{si}) and 10m wind speed (v_a). p represents the proportion of iceberg simulation time steps during which specific characteristics (e.g. $CI > 15\%$) are observed. Time steps and grid cells in which the variable does not influence iceberg drift and deterioration (e.g. heavy sea ice conditions for v_w) are excluded.

Variable	Topaz
$\varnothing SST\,[°C]$	-0.85
$\varnothing v_w\,[m\,s^{-1}]$	0.06
$\varnothing CI\,(CI > 15\%)\,[\%]$	86
$\varnothing h_{si}\,(CI > 15\%)\,[m]$	0.57
$p(CI > 15\%)\,[\%]$	53
$\varnothing v_{si}\,(CI > 15\%)\,[m\,s^{-1}]$	0.09
$\varnothing v_a\,[m\,s^{-1}]$	6.61

Variable	ERA5 ~~has a regular latitude-longitude grid (Hersbach et al., 2020) and the search radius varies with the latitude according~~
$\varnothing v_a\,[m\,s^{-1}]$	6.69

~~The simulations of iceberg drift and deterioration are influenced by the availability of the environmental forcing data (Bigg et al., 1997; Kub and data assimilation approach in the iceberg model (Herrmannsdörfer et al., 2024). In the following Section, the spatial availability of the forcing variables is analysed for the iceberg model setup (Sect. 2.3) and the different forcing datasets (Sect. ??).~~ ***Sea ice***

~~The iceberg model assimilates environmental data at every simulation time step from the nearest grid cell of the forcing data grid (*nearest forcing cell*) or averages the surrounding grid cells (*neighbour average*) with an increasing search radius sr (Sect. 2.3, Eq. **??**). We investigate the relative number of simulated iceberg trajectories and simulation time steps that used nearest neighbour or neighbour average of a certain radius. Note that we differentiate the usage (of e.g. neighbour average of radius 1)~~ We find that CI and h_{si} are on average 4% and $0.84\,m$ larger in Barents-2.5, compared to Topaz, within the sea ice edge ($CI > 15\%$) in the iceberg pathways (Tab. 2). Some of the largest differences between the sea ice models are present along the typical spring sea ice edge, especially around northern Svalbard (Fig. 2). Sea ice ($CI > 15\%$) also occurs in 23% more time steps in the iceberg pathways in Barents-2.5 as the southward extent of light and heavy sea ice is larger. Previous studies describe an underestimation of sea ice area, CI and h_{si} (especially along the sea ice edge) in Topaz (Xie et al., 2017; Xie and Bertino, 2022) and general overestimation, but skilful CI, in Barents-2.5 (Röhrs et al., 2023). Topaz CI is found to be closer to the observations as the Barents-2.5 hindcast (Idžanović et al., 2024). Further analysis in this study

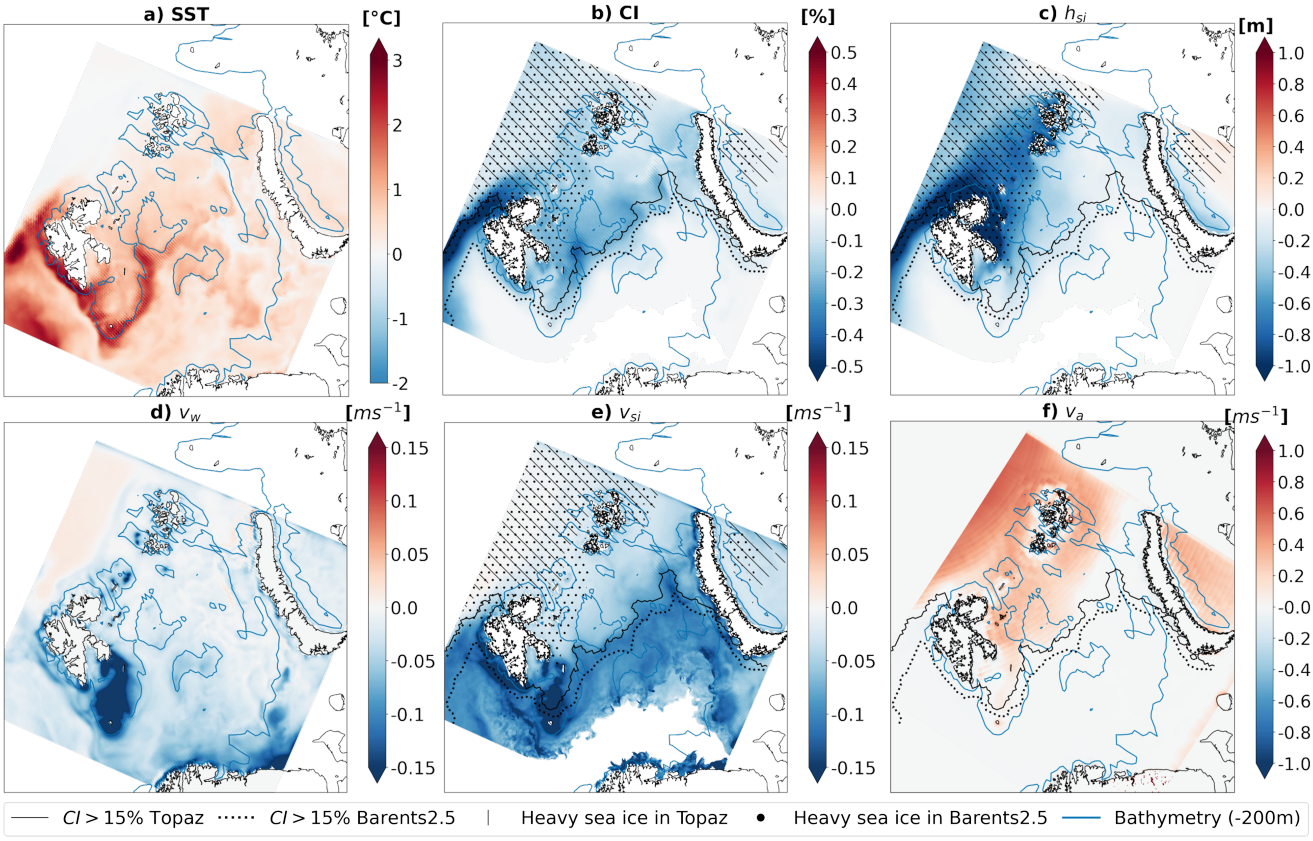

Figure 2. Spatial ~~assimilation of gridded environmental data into~~ differences in ocean, sea ice and atmosphere variables in the ~~iceberg~~ model. ~~At every simulation time step~~ Barents Sea in Topaz, Barents-2.5, ERA5, and CARRA, namely (~~numbers~~a) SST, ~~triangles~~(b) ~~of the iceberg trajectory~~ CI, (~~white line~~c) h_{si}, ~~the environmental data is assimilated from the nearest forcing grid cell~~ and total speeds of (~~*nearest forcing cell*~~d) v_w, ~~green circles~~(e) ~~. The distance is estimated between iceberg~~ v_{si}, and ~~grid cell centre~~ (~~green lines~~f) v_a. ~~If~~ Shown for comparison, the ~~nearest forcing cell does not contain data~~ -200, m bathymetry isolines (~~e.g. over land~~blue lines), the average ~~is calculated from the surrounding available forcing cells~~ April sea ice edge (~~*neighbour average*~~$CI > 15\%$, ~~pink~~ black lines), ~~squares~~ and ~~circles). Note~~ the ~~depiction~~ extent of ~~the coastline~~ heavy sea ice (~~brown line)~~$CI > 90\%$, ~~ocean (blue dots and background~~$h_{si} \geq h_{min}$, hatches) for 2010–2014 and ~~land grid cells (brown dots and background).~~2020–2021.

(not shown) revealed large differences between the sea ice variables in ~~the iceberg trajectories, and simulation time steps , aggregated from all simulated iceberg trajectories.~~

~~Figure **??** visualises the horizontal grid resolution of the forcing data sets, the search radius and how often it is used in~~ Topaz~~-~~, Barents2Barents-2.5 ~~-~~, ERA5~~- and CARRA-forced iceberg simulations. The x-axis shows the maximum search radius *sr*, which represents the maximum distance of an iceberg to the closest grid cell centre with available forcing data. The y-axis shows how often forcing is aggregated at the maximum search radius on the x-axis. Note, that the percentage changes step~~

wise along the x-axis corresponding to the respective grid resolution. The plot elements show the percentage of available data relative to the number of iceberg trajectories (bars) , simulation data points (time steps aggregated from all trajectories) in which all variables are available (lines)in the differently forced simulations (colours)forecast (used 2020-2021), which is constrained to sea ice observations, and the Barents-2.5 hindcast (used 2010-2014), which is a free-run. Further analysis (not shown) also revealed that the SST and sea ice differences vary seasonally. Compared to the known too fast decline and freeze-up in Topaz (Xie et al., 2017; Xie and Bertino, 2022), we found that the melt season is delayed and the sea ice advance is similar in Barents-2.5.Note that the numbers do not add up to , as different variables, or time steps within a trajectory, are often acquired from different search radii.

Acquisition (, y-axis) of different environmental forcing data (colours) in the iceberg simulations and distance of acquisition (x-axis). The iceberg model assimilates environmental forcing from the forcing data's grid cell with the smallest distance to the current iceberg position (nearest neighbour approach, see Sect. 2.3 and Fig. **??**). In the case of unavailable forcing in the nearest forcing cell, data is averaged from the surrounding grid cells of increasing search radius. The availability of forcing data (, y-axis) is given as function of the maximum search radius (or maximum distance between iceberg and grid cell centre) (x-axis), that changes step wise dependent on the horizontal data resolution. The availability is given for the datasets of Topaz (blue), Barents (green), ERA5 (orange) and CARRA (red). The availability is given relative to the number of iceberg trajectories (bars) and simulation time steps (lines).

Availability of data in the nearest forcing cell*Ocean and sea ice velocity*

In generalThe sea surface and sea ice speeds are on average $0.05\,\mathrm{m\,s^{-1}}$ and $0.02\,\mathrm{m\,s^{-1}}$ larger over the iceberg pathways in Barents-2.5 (Tab. 2, Fig. **??** shows, that in the majority of trajectories ()2). The v_w differences are particularly large in coastal and shallow areas (between Svalbard and Franz-Josef-Land, around Svalbard, Spitsbergen Bank, and Central Bank).The differences are smaller in open ocean. The v_si differences are largest around the sea ice edge ($CI \approx 15\%$) and the majority of time steps (), the forcing variable(s)are available in the nearest forcing cell.

Neighbour averagingThe neighbour average is applied (due to missing data in the nearest forcing cell) in all differently forced simulations, however the frequency of occurrence and the search radius differ in the simulations with varied forcing. of Topaz- and of south-western Svalbard. In contrast, Topaz has larger water and sea ice speeds towards the Eurasian Basin. In contrast to Topaz, Barents-2.5 -forced trajectories, and of Topaz- and of accounts for the effects of air pressure and tides on the water velocity, and represents local water velocities due to its high horizontal and temporal resolution. Model skill varies over time and spatial scales, and low predictive skill for surface water speed and direction in Barents-2.5 -forced time steps, require neighbour averaging for some variable and time step. Further investigation (not shown) indicated that the availability of Barents-2.5 variables differs is due to the variable's native grid upon production.

Search radiiFor most of the neighbour averages, a search radius of 1 forcing cell is sufficient. Larger search radii are necessary with decreasing frequency. Around () of the Topaz and () of the Barents2.5-forced trajectories, but only of the Topazand of chaotic nature of the system, the scarcity of observations and error statistics. Some skill can be accounted to water velocities in mainly wind-driven conditions, and the Barents2.5-forced time steps, use search radii larger than one cell (and

~~respectively). The largest applied search radius was 3 forcing cells () for Topaz and 4 forcing cells () for~~ sea ice velocity. The speeds have a positive bias (Röhrs et al., 2023; Röhrs et al., 2023; Idžanović et al., 2023). Lower horizontal resolution ocean models, such as Topaz, have smaller gradients and lower velocities in general. Topaz also shows issues with simulating the circulation of Atlantic water inflow and the topographically-steered currents. Note that, in Tab. 2 and Fig. 2, the diurnal tidal cycle largely cancels out in the water velocity average and it's difference in Topaz and Barents-2.5. ~~Further studies~~ However, Figure 2 still shows the differences due to other processes (e.g. topographically-steered currents). Further analysis (not shown) ~~indicated that Barents-2.5 sea ice velocity is partly unavailable within a larger search radius~~confirmed large differences for hourly time steps in shallow areas such as Spitsbergen Bank) due to tidal representation.

~~Availability of wind data~~10m Wind

~~The availability of wind forcing in the nearest forcing cell is higher than for the other forcing variables and is available within a search radius of 3 cells or less for both~~ In the iceberg pathways of the Barents Sea, the average wind speed difference between ERA5 ~~(not given in km)~~ and CARRA ~~()~~ ($+0.08\,\mathrm{m\,s^{-1}}$) is relatively small compared to the ~~approximate resolution in the Arctic of~~ absolute wind speeds (⌀ $6.60\,\mathrm{m\,s^{-1}}$ to $6.69\,\mathrm{m\,s^{-1}}$) and varies just as much as in the pathway differences by the ocean and sea ice input. Differences are especially small over open waters and are locally larger along the coastlines with complex topography. In previous studies, CARRA was found to provide added value over ERA5, especially over complex topography and sea ice, due to its improved physical parametrisation and higher resolution satellite observations of sea ice (Køltzow et al., 2019, 2022; Giusti, M., et al., 2024). We highlight larger average wind speeds in ERA5 in the northern, frequently sea-ice-covered part of the domain and larger speeds in CARRA in the southern, water-covered part of the domain in Fig. ~~??.~~ 2, that are likely due to different representation of surface roughness over water and sea ice, or prescription of different CI products (Hersbach et al., 2020; Yang et al., 2020; Giusti, M., et al., 2024).

3.1 ~~Iceberg deterioration~~

~~The iceberg deterioration accounts for wave erosion, buoyant vertical convection and basal melt in this setup(Sect. 2.3)~~We highlight that similarities (e.g. in ERA5 and CARRA wind) partly result from the interconnection of the described environmental models by the use of the respective other models (or different version of a similar setup) at the ocean, sea ice and atmosphere interface and the lateral boundaries (e.g. CARRA using ERA5 at lateral boundary and surface or Topaz using ERA5 at the surface).

4 Analysis of the iceberg simulation results

4.1 Iceberg drift and deterioration

In this section, we compare the distance along the trajectory (*Track*), the shortest distance between seeding and the melt position (*Effective*) and the time an iceberg persists until it is melted (*Duration*). Further we analyse the relative contributions of the various melt terms. ~~The deterioration Eq. are described in detail in the Appendix.~~

The total iceberg deterioration rate of an iceberg in simulation time step j (with length $dt = 3600 \cdot 2\,\mathrm{s}$) is ~~measured~~ calculated as mass loss or reduction in volume ~~times~~ multiplied by the density ρ_i of glacial ice (Eq. ~~??).~~ 1).

$$\delta_j = m_{j+1} - m_j = \rho_i \cdot (H_{j+1} \cdot W_{j+1} \cdot L_{j+1} - H_j \cdot W_j \cdot L_j) \tag{1}$$

$$= \rho_i \cdot ([H_j + \Delta H_j] \cdot [W_j + \Delta L_j] \cdot [L_j + \Delta L_j] - H_j \cdot W_j \cdot L_j) \tag{2}$$

where ~~$\Delta H_j = M_{\mathrm{fb}} \cdot dt$~~ $\Delta H_j = M_{\mathrm{fw}} \cdot dt$ is the reduction in height during time step due to melt at the base (M_{fw}). $\Delta L_j = \Delta W_j = (M_{\mathrm{e}} + M_{\mathrm{v}}) \cdot dt$ is the reduction at the sides due to wave erosion (M_{e}) and vertical buoyant convection (M_{v}).

~~We introduce the measure of the relative contribution of a melt term~~ Equation 3 introduces the contribution of each melt term relative to the total deterioration (~~δ~~$\delta(term)$, in %)

$$\delta = \frac{\sum_{j=1}^{J} \delta(j, term)}{\sum_{j=1}^{J} \delta(j)} \cdot 100\%$$

~~where~~ . i and j ~~is any simulation time step~~ are counters of icebergs and time steps, respectively. I and J ~~is the number of simulation time stepsof 2603 · 7 icebergs of similar environmental forcing. The contribution δ by wave erosion is largest~~ are the the total number of simulated icebergs and time steps, respectively.

$$\delta(term) = \frac{\sum_{i=1}^{I} \sum_{j=1}^{J} \delta(i, j, term)}{\sum_{i=1}^{I} \sum_{j=1}^{J} \delta(i, j)} \cdot 100\% \tag{3}$$

Wave erosion $\delta(M_e)$ contributes most ($55 - 74\%$), followed by basal melt $\delta(M_{fw})$ ($25 - 44\%$) (~~) , and vertical convection () (Table~~ Tab. 3). However, the relative importance of the deterioration terms varies with the environmental ~~forcing~~data. Comparing the ~~differently forced simulations , Topaz-forced icebergs~~ simulations with different environmental input, icebergs with Topaz input have larger wave erosion ($+19\%$) and smaller basal melt (-19%). The ~~difference~~ relative contribution in vertical convection ~~is small, as the relative contribution. Further studies (not shown) indicated a larger mass loss averaged~~ $\delta(M_v)$ and its difference with environmental input is small. The average mass loss over all time steps ~~in Topaz-forced simulations . It also showed~~ is $6.2 \cdot 10^4$ kg larger in simulations with Topaz input. Further studies (not shown) indicated small melt rates for times steps in sea ice. An example of the relative contributions of the deterioration terms and their ~~deviations for differently forced simulations is also~~ differences for simulations with different environmental input is given in Sect. 4.4.

4.2 ~~Iceberg drift duration and distance~~

Table 3. ~~Contribution to~~ Total iceberg deterioration and the contribution from different ~~forcing~~ deterioration terms (wave erosion M_e, basal melt M_{fw} and vertical buoyant convection M_v) in ~~Topaz~~ simulations using Topaz and Barents-2.5 ~~forced simulations~~, and their difference. The values are expressed as average total deterioration ($\varnothing\delta$, in 10^4 kg) and relative contribution to the total mass loss or deterioration (~~δ, in %~~$\delta(M,\%)$). Note that $\delta(M_v)$ is given with higher precision to show its difference with ocean input.

	$\varnothing\delta$	$\delta(M_e)$	$\delta(M_{fw})$	$\delta(M_v)$
Topaz	18.2	74	~~27~~ 25	0.8
Barents-2.5	12.0	55	~~43~~ 44	0.6
Topaz-Barents2.5	+6.2	+19	~~-17~~-19	+~~0.1~~0.2

~~This Section examines how the drift duration and distance are influenced by the selection of ocean, sea ice and atmosphere forcing, for a range of seeding conditions. In detail, the distance along the trajectory (*Track*), the distance between seeding and the melt position (*Effective*) and the time, in which an iceberg persists until it is melted (*Duration*), are analysed.~~

~~Comparing simulations of~~ In simulations with different ocean and sea ice ~~forcing, Topaz-forced icebergs drift in average shorter~~in time inputs, icebergs with Topaz input drift on average 8 days duration shorter, 18 km less in distance along the track, but 6 km more in effective distance (Fig. 3). These differences are partly relevant as they make up 28%, 5% and 6% of the mean absolute values of all simulations. The difference between simulations with ~~varied atmospheric forcing~~ varying atmospheric input are minor.

The iceberg drift duration and distance also vary ~~from source~~by source, and its seeding characteristics (number and size) (Fig. 3). The dependency on the seeding location causes a variation of 8 to 62 days, 140 to 594 km (Track) and 61 to 146 km (Effective). Iceberg drift duration and distances (Track, Effective) are highest for icebergs originating from Franz-Josef-Land and Austfonna, and smaller for Edgeøya and Novaya Zemlya in all simulations.

Analysing the dependency on both source and ~~forcing~~environmental input, the differences between the sources ~~dominate~~ is larger than the difference due to the ~~forcing~~ environmental input (Fig. 3). Similarities and differences ~~between the~~ in iceberg drift from various sources are ~~to a large extent~~ largely reproduced by the ~~differently forced simulations~~ simulations with different environmental input. However, differences between ~~Topaz~~ drift under Topaz and Barents-2.5 ~~-forced drift~~ input are significant and vary in both ~~sign and magnitude. The drift distance (Effective, Track) of Topaz-forced trajectories is longer for icebergs originating~~ positive and negative magnitudes. For example, icebergs with Topaz input from Franz-Josef-Land ~~and Novaya Zemlya, while it is shorter for icebergs from Austfonna and Edgeøya. The drift durationis shorter for Topaz-forced simulations. The difference due to varied atmospheric forcing is minor.~~drift on average larger distances, but in a shorter duration.

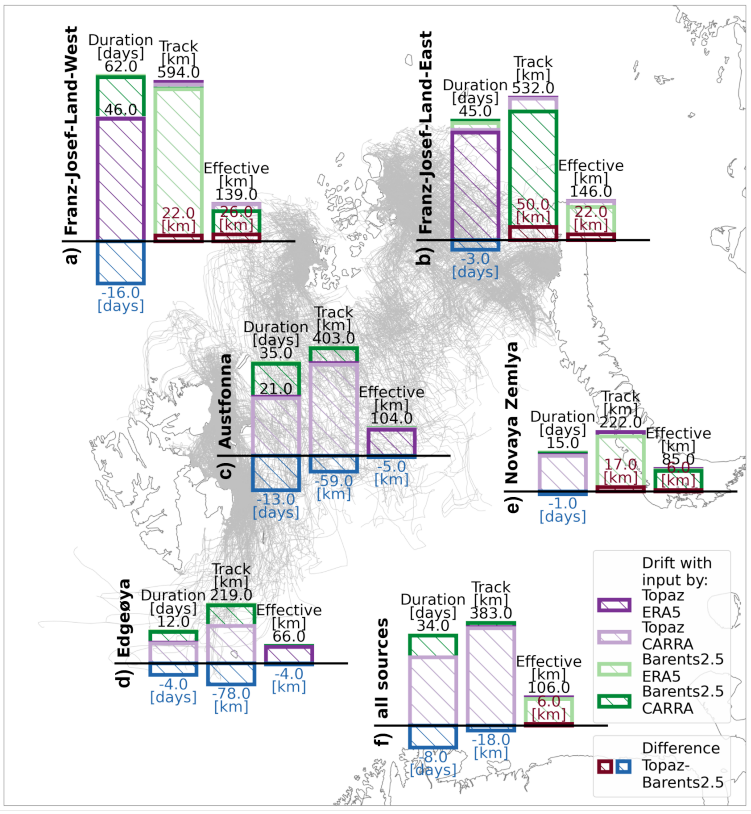

Figure 3. Average drift duration [days], distance (Track, Effective) [km] for icebergs originating from the sources Franz-Josef-Land West and East (a,b), Austfonna (c), Edgeøya (d) and Novaya Zemlya (e), and their combination (f). Drift statistics are given for simulations using different environmental input (green and purple bars) and their difference (red and blue bars)

~~Average iceberg drift duration and distance (Track, Effective) and their difference under varied forcing (y-axis) for differently forced iceberg trajectories (colours), originating from the sources Franz-Josef-Land East and West, Austfonna, Edgeøya and Novaya Zemlya (x-axis).~~

4.2 Spatial iceberg density

Iceberg density is a measure ~~to express~~ of the average number of icebergs in a domain over a time period, along with the number of simultaneous occurrences. ~~In this study, the iceberg density is compared for the differently forced simulations to analyse the spatial differences in iceberg drift and deterioration.~~

The iceberg density is derived ~~by~~ from the number of icebergs i that are within a defined grid cell at the same simulation time step, the number of time steps n in which i icebergs are within the same grid cell and the total number of simulation time steps ~~N~~J. The probability of having i icebergs in one grid cell at same time step $p(i)$ is calculated for every occurring i by

Eq. 4. The areal density ρ_a (~~called~~ referred to as *iceberg density* ~~in the following~~hereafter) is given by Eq. 5 with the surface area of the grid cell A_{gridcell}. The unit of ρ_a is "number of icebergs per area and time step". In this analysis, iceberg density is ~~accumulated~~ aggregated on an artificial grid of 25 km horizontal resolution~~.~~ , similar to a curvi-linear Topaz grid at reduced resolution. Apparent iceberg occurrences on land result from accumulating occurrences on this grid.

$$p(i) = \frac{n(i)}{N} \frac{n(i)}{J} \tag{4}$$

$$\rho_a = \frac{\sum_{i=0}^{\infty} i \cdot p(i)}{A_{\text{gridcell}}} \tag{5}$$

Figure 4 shows maps of the iceberg density in the Barents Sea for the ~~differently forced simulations . The colour scale in Fig. 4 supports the data below the 95th percentile of the densities (grey,) and the highest (orange colouring and white line, individual for every simulation).~~ simulations with different environmental input. Iceberg densities are highest ~~(largest , white line and orange colour map in Fig. 4)~~ around eastern Svalbard, Franz-Josef-Land and northwestern Novaya Zemlya ~~(Sect. 2.3)~~ and decreases with increasing distance to those locations~~, independent of the forcing~~.

Figure 5 shows the spatial density differences between the ~~differently forced simulations~~ simulations with different environmental input. Density differences are as large as absolute densities, which is highlighted by similar density range in Fig. 4 and 5. Deviations by varied ocean and sea ice ~~forcing~~ input are larger than deviations by varied atmospheric ~~forcing~~input, however some effects of ocean and atmospheric ~~forcing~~ input add up while some cancel each other out.

Simulations of varied ~~ocean- and sea ice-forcing~~ ocean and sea ice input show significant difference in large parts of the domain, and especially around Svalbard and Franz-Josef-Land (Fig. 5). Thereby, ~~Topaz-forced simulations~~ simulations with Topaz input have higher density ~~close to~~ near the coastline of Franz-Josef-Land and Svalbard, and lower density in ~~larger proximity of~~ farther from the archipelagos. The density differences are decreasing towards the open ocean.

~~A selection of regional density difference from Fig. 5 is noted in the following. Iceberg densities are larger for~~ We also highlight the larger density for simulations with Barents-2.5 ~~-forced simulations~~ input in the northernmost parts of the domain~~. Iceberg density is higher to the north and west (south) of the main iceberg source on Novaya Zemlya for~~ , and the higher density to the northwest (northeast) of Bjørnøya for simulations with Topaz (Barents-2.5) ~~-forced simulations. For more, iceberg density is larger to the north-west (north-east) of Bjørnøya for Topaz (Barents-2.5)-forced simulations.~~input. Density differences due to atmospheric input are small across most of the domain, but can be in the scale of the absolute values regionally.

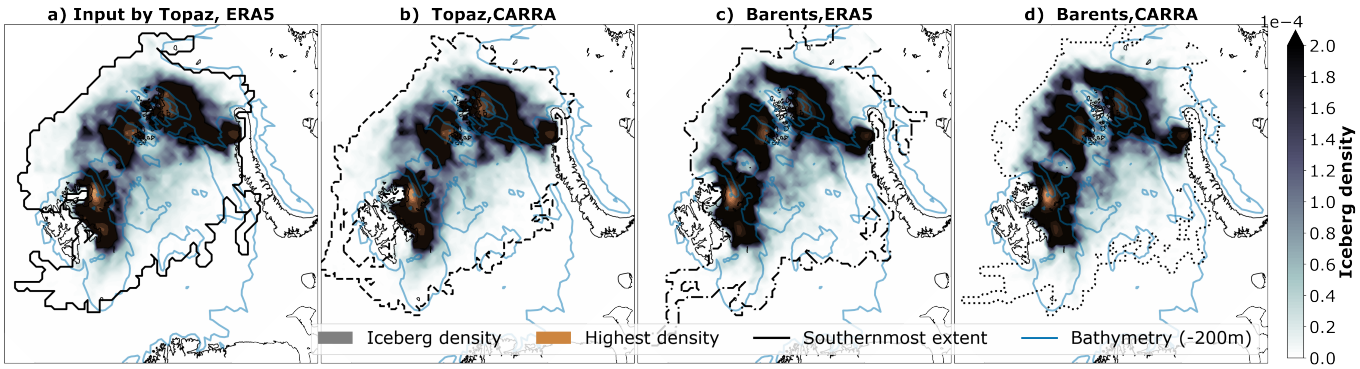

Figure 4. Iceberg density (colours) and southernmost extend (black line), aggregated ~~for~~ from simulations ~~forced by~~ using a) Topaz and ERA5, b) Topaz and CARRA, c) Barents-2.5 and ERA5 and d) Barents-2.5 and CARRA. ~~The largest of the respective simulations' iceberg density is~~ Highest densities are highlighted ~~(white line, in~~ orange colour~~map)~~.

4.3 ~~Iceberg~~ Spatial and seasonal iceberg extent

The iceberg extent is a measure of how far icebergs drift, how much they spread and how much they are restricted to common pathways. The maximum spatial iceberg extent is ~~shown by~~ indicated by the black lines in the Fig. 4 ~~. All simulated icebergs in the accumulated time period 2010-2014 and 2020-2021 drifted within the indicated lines. Icebergs in Barents-2.5-forced simulations show larger spread in the domain, in all directions (Fig. 4). In contrast, Topaz-forced icebergs drift further north and west from Svalbard.~~ and 5 and shows little difference across varied environmental input.

More detailed analysis (not shown) indicates that the southernmost iceberg trajectories reach ~~to the~~ south of Bjørnøya and to the south-eastern Barents Sea around $72-74°$N, ~~independent on the forcing~~regardless of the environmental input. Some of ~~those~~ these icebergs drift within sea ice of high concentration~~and some~~ , while others drift in open waters. The southernmost trajectory reached 72°N in the Central Basin for ~~the~~ simulations with Barents-2.5 ~~-forced simulations and is~~ input, as described in Sect. 4.4.

~~The iceberg extent can also be described by~~ We adapt the definition of the iceberg extension from Keghouche et al. (2010) and show the relative number of grid cells ~~that contain~~ containing icebergs at a given time ~~step, the iceberg extension. In the following, the iceberg extension is analysed as time series from 2010 to 2014 and 2020 to 2021 (~~in Fig. 6~~)~~. The iceberg extension varies ~~in~~ with time and between the ~~differently forced simulations (Fig. 6).~~ simulations with different environmental input. The iceberg extension varies ~~for simulations with~~ in simulations with both different atmospheric and ocean-sea ice ~~forcing~~input, and at ~~a similar scale~~the same amplitude.

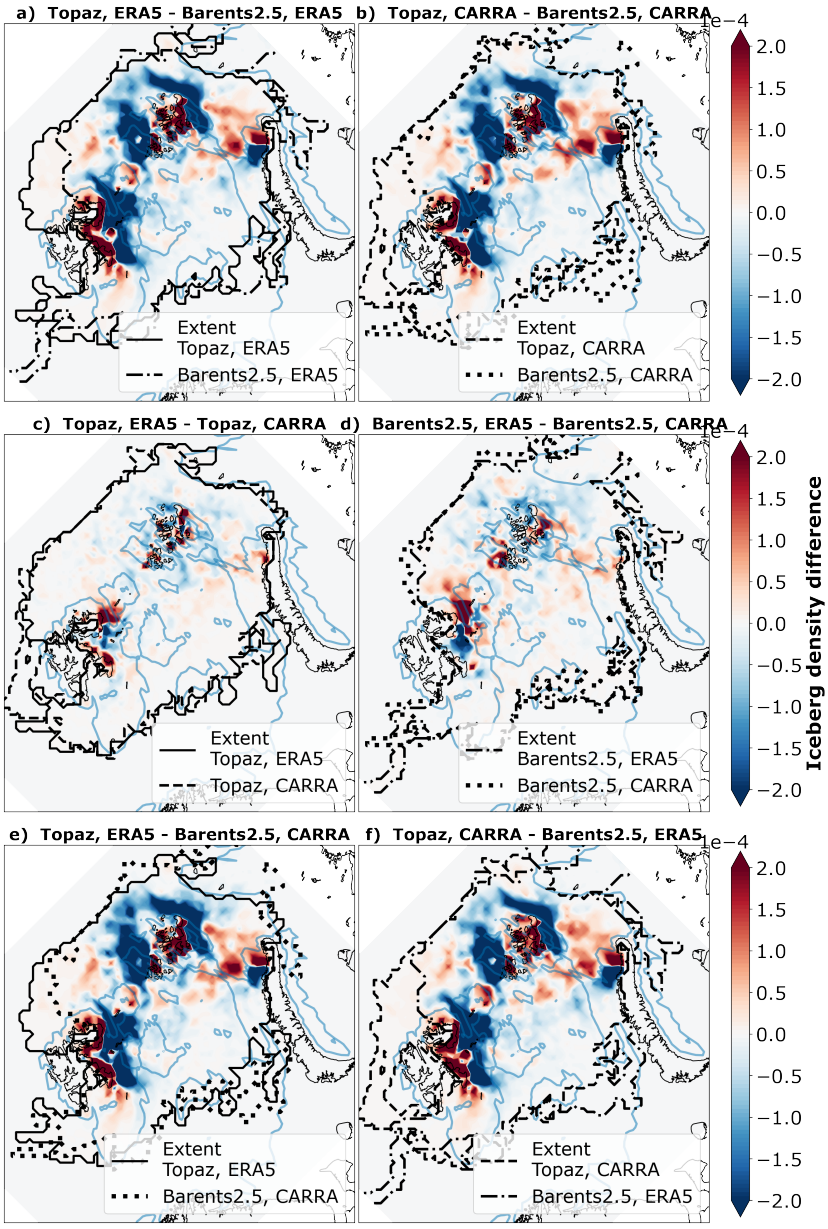

Figure 5. Difference of iceberg density (colours) and southernmost extend (lines) in simulations with a,b) varied ocean and sea ice ~~forcing~~input, c,d) varied atmospheric ~~forcing~~ input and e,f) variations of both ~~forcing datasets~~environmental inputs.

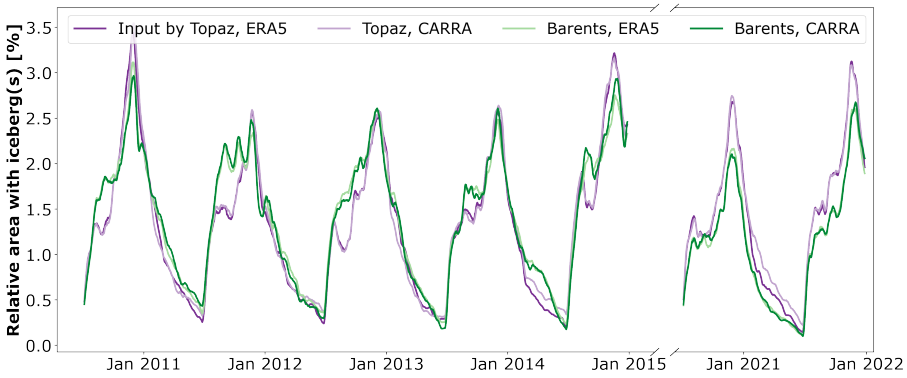

Figure 6. Time series of iceberg extension ~~(relative number of grid cells containing icebergs,~~ in ~~of all grid cells) in~~ the ~~differently forced~~ iceberg simulations with different environmental input (colours) from 2010 to 2014 and 2020 to 2021. The extension is relative to the number of artificial analysis grid cells with a horizontal resolution of 25 km. A 10 days rolling average ~~has been~~ is applied.

In detail, the iceberg extension ~~has~~ follows a seasonal cycle and exhibits multi-year variability (Fig. 6). This variability is ~~reproduced in all differently forced simulations , however~~ visible in all simulations with different environmental input, although with small deviations. The iceberg extension increases from July to December, when icebergs are seeded, and then decreases again until July. The period ~~of~~ from July to December is characterised by large ~~deviation~~ deviations with varied ocean ~~forcing~~ input and small variations with atmospheric ~~forcing~~input. Largest differences with varied ocean and sea ice ~~forcing occur in~~ input occur from August to September and November to December. The period from December to June shows similar deviations with varied ocean and atmospheric ~~forcing~~input. These deviations are differently pronounced in ~~the~~ individual years of the ~~timeseries (Fig. 6).~~ time series.

4.4 Example of an iceberg trajectory

~~The iceberg(~~This Section presents an illustrative example of the drift and deterioration of the synthetic iceberg, referred to as *iceberg 2013-788*~~) drifted southward from Franz-Josef-Land from autumn 2013 to spring 2014 (Fig. 7).~~ . The trajectory of iceberg *2013-788* is ~~some~~ one of the longest (up to 249 days, 1030 km effective and 3900 km track distance) and southernmost trajectories (down to 72°N) ~~out of~~ amongst the statistics of ~~2603 · 7 · 4~~ 72884 simulated trajectories discussed in this study (~~Table~~ Tab. 4). The exceptionally long drift is caused by an above average initial size and initial position far north. As such, the example is not suitable for explaining the average differences in iceberg simulations with varied environmental input, but serves as illustration of the impact of environmental input.

The iceberg drifted southward from Franz-Josef-Land between autumn 2013 to spring 2014 (Fig.7). Trajectories with different ocean and sea ice ~~forcing~~ input deviate significantly in the second half of the drift, ~~drifting~~ leading into the Central Basin under Barents-2.5 ~~forcing~~ input and into the Hopen Trench under Topaz ~~forcing (Fig. 7). The~~ input. The icebergs with

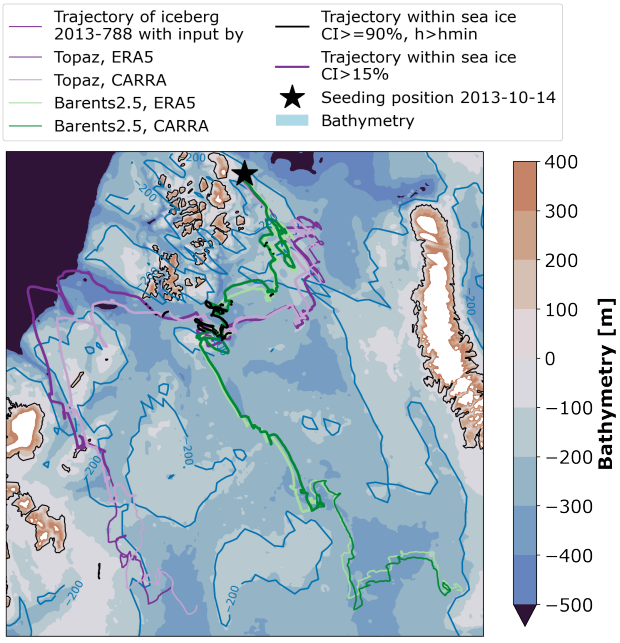

Figure 7. Simulated drift of *iceberg 2013-788*, seeded at the 14 October 2013, close to north-eastern Franz-Josef-Land (star). The trajectories correspond to simulations of iceberg drift and deterioration with varied environmental ~~forcing~~ input (coloured lines). Along the trajectories, ~~weekly time steps (black squares) and~~ simulation time steps ~~with relevant~~ in light sea ice ($CI > 15\%$, thicker lines) and heavy sea ice conditions ($CI \leq 90\%$ and ~~$h_{si} > h_{min}$~~ $h_{si} > h_{min}$, black lines) are marked.

Table 4. Characteristics of the drift of *iceberg 2013-788*. Iceberg drift ~~duration~~ *duration* [days], ~~effective~~ *effective* drift distance [km], drift distance along the trajectory [*Track*, km], southern-most latitude [*min lat.* °N] and simulation end date (*Melt date*).

~~Forced by~~ Env. input	Duration [days]	Effective dist. [km]	dist. Track [km]	min lat. [$^\circ N$]	Melt date
Topaz, ERA5	249	936	3852	75.5	2014-06-20T06
Topaz, CARRA	229	968	3401	75.0	2014-05-31T04
Barents2.5, ERA5	236	1038	3204	72.0	2014-06-06T12
Barents2.5, CARRA	232	1031	3209	72.1	2014-06-03T08
Topaz - Barents2.5	+11	-82	+420	+3.2	-
ERA5 - CARRA	+23	-12	+223	-0.3	-

Barents-2.5 ~~trajectory~~ input drifted 3° further south (~~Table~~ Tab. 4). The ~~Topaz-forced trajectories~~ trajectories with Topaz input have a longer drift duration (+11 days) and distance along the track (+420 km), but a shorter effective drift distance (−82 km). The trajectories show minor deviations due to varied atmospheric ~~forcing on the large scale~~input.

425

The environmental conditions in the Barents Sea are shown for selected time steps during the winter 2013-2014 in Fig. 8. The environmental ~~forcing~~ input along the trajectory of *iceberg 2013-788* is shown as timeseries in Fig. 9.

~~Relevant sea ice~~ At the seeding time in mid-October 2013, sea ice ($CI > 15\%$) is restricted to the north and west of Franz-Josef-Land in Topaz~~at the seeding time in mid October 2013.~~. At the same time, sea ice in Barents-2.5 encloses the archipelago, setting the iceberg in light sea ice conditions (line hatches in Fig. 8). During the winter, the ~~relevant~~ sea ice expands south-east-ward, with light sea ice reaching as far south as Hopen island for Topaz and as far south as Bjørnøya for Barents-2.5 in late April. The cover of heavy sea ice is larger in Barents-2.5 throughout the winter (Fig. 8, point hatches). The sea surface temperature reflects this difference in the spatial distribution accordingly.

Along the trajectory, the icebergs drift within ~~sea ice (relevant for iceberg drift)~~ the sea ice edge $70 - 77\%$ of the simulation days (~~Table~~ Tab. 5, Fig. 9). ~~Thereby~~ Simulations with Barents-2.5 ~~forced simulations~~ input show a larger number of days with ~~relevant~~ sea ice ($+7\%$ of days), average 10% larger CI and $0.1\,\mathrm{m}$ larger h_{si}. The SST is on average $0.01°\mathrm{C}$ larger in trajectories with Topaz input (Tab. 5). The SST along the trajectory is characterised by the present sea ice until April/May 2014 ($\approx -2°\mathrm{C}$) and followed by the drift into warmer Atlantic waters (up to $+4°\mathrm{C}$) in the Hopen Trench and the Central Basin (Fig. 7, 9). ~~The~~

We highlight the period between 1 April and 15 May 2014, when the icebergs drift out of the sea ice edge, to the east of Svalbard (Topaz input) and in the Central Basin (Barents-2.5 input). The general environmental situation in April 2013 can be described by the yearly maximum sea ice extent and infusions of warm Atlantic waters towards the sea ice edge (e.g. along the Hopen Trench and Central Basin) (Fig. 8). Along the trajectories, the icebergs face decreasing sea ice concentration and thickness and increasing SST ~~is in average larger in Topaz-forced trajectories(Table 5).~~ during their southward drift (Fig. 9). The icebergs also face rapid changes in wind and water speed.

Wind, sea water and sea ice speed vary across the domain and fluctuate on short temporal scales in the timeseries, especially for Barents-2.5, ERA5 and CARRA (Fig. 9). ~~The speed of the forcing variables is in average larger in Barents-2.5 () for water, for sea ice, Table 5). Further analysis~~ Further analysis (not shown) obtained that the wind speed deviates to a larger degree for varied ocean ~~forcing~~ input (position) than atmospheric ~~forcing~~ input (wind speed itself~~,~~).

The iceberg deterioration rate is small ($20 \cdot 10^4\,\mathrm{kg\,2h^{-1}}$) during the drift within sea ice, and basal melt dominates (Fig. 9, means not shown). When the icebergs start to drift outside of the sea ice, the deterioration rates increase ($89.5 \cdot 10^4\,\mathrm{kg\,2h^{-1}}$) and the contribution by wave erosion dominates (not shown). Note that the deterioration rate decreases with decreasing iceberg size. The total deterioration rate of *iceberg 2013-788* is on average $0.9 \cdot 10^4\,\mathrm{kg\,2h^{-1}}$ smaller in trajectories with Barents-2.5 input (Tab. 6). On average, the contribution by wave erosion is larger in trajectories with Topaz input ($+5\%$), compared to Barents-2.5 input. The opposite is true for the basal melt (-5%). Further analysis

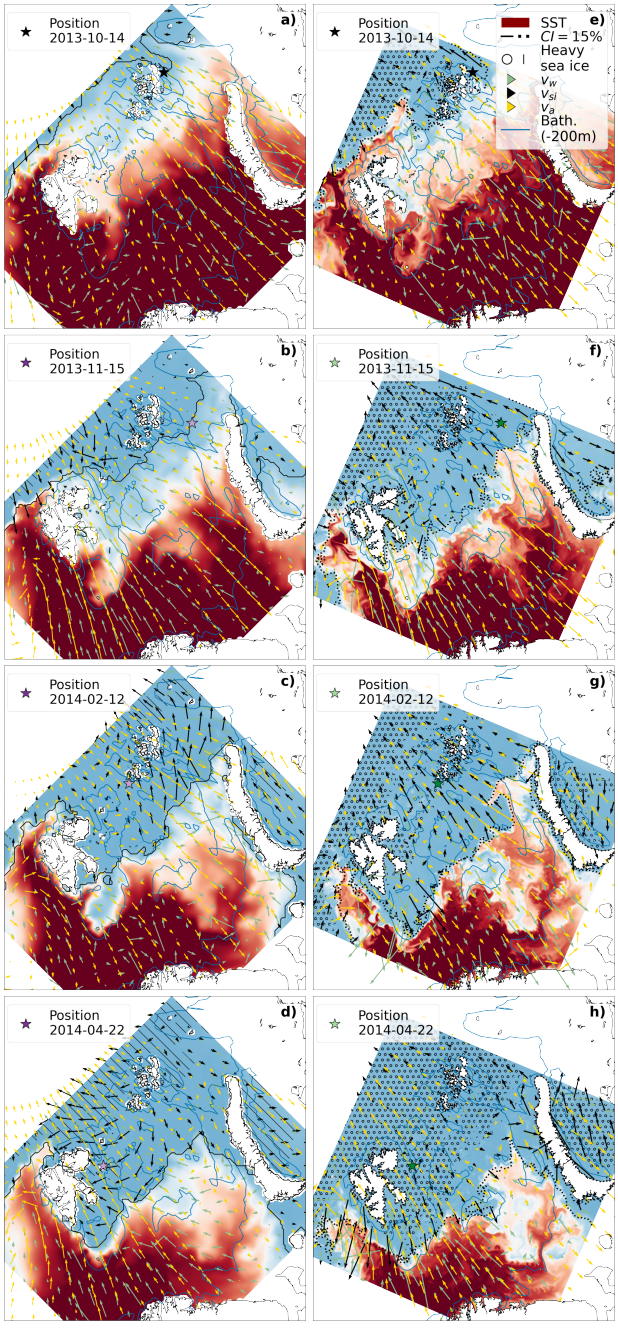

Figure 8. Environmental conditions in the Barents Sea at the 14 October 2013 (a,e), 15 November 2013 (b,f), 12 February 2014 (c,g) and 22 April 2014 (d,h). Ocean and sea ice conditions are ~~given~~ provided by Topaz (a-d) and Barents-2.5 (e-h). The atmospheric conditions are provided by ERA5 (a-d) and CARRA (e-h). Shown variables are the sea surface temperature (contour colours), ~~light~~ sea ice edge ($CI > 15\%$, black line~~hatches~~), heavy sea ice (~~$CI \leq 90\%$, $h_{si} > h_{min}$~~$CI \leq 90\%$, $h_{\mathrm{si}} > h_{min}$, ~~point~~ hatches), as well as momentary sea ice drift (black arrows), sea surface velocity (green arrows) and 10m-wind (yellow arrows). Note ~~,~~that the directional data is given for reduced (approx. 100 km resolution) for increased visibility. The respective position of *iceberg 2013-788* (star) is marked for the simulations ~~forced by~~ using Topaz ~~and ERA5~~ (~~Blue~~purple) ~~, Topaz~~ and ~~CARRA (orange),~~ Barents-2.5 ~~and ERA5~~ (green)~~and Barents-2.5 and CARRA (red)~~.

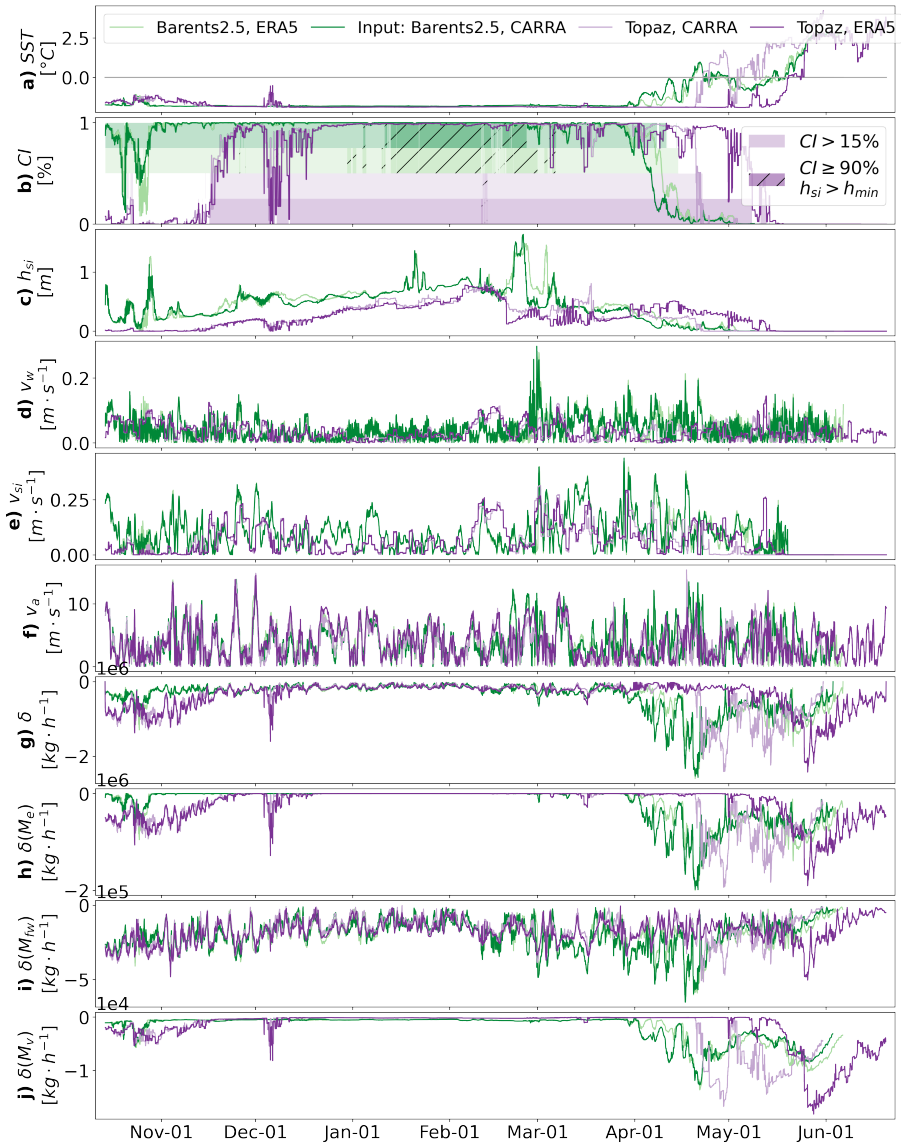

Figure 9. Time series of iceberg and ~~forcing~~ environmental characteristics along the trajectory of *iceberg 2013-788*. Environmental ~~forcing~~ input along the trajectory with a) sea surface temperature SST [°C], b) sea ice concentration CI and time steps with $CI > 15\%$ (colour) and $CI \leq 90\%$ with $h_{\mathrm{si}} > h_{\mathrm{min}}$ (colour, hatches), c) sea ice thickness ~~h_{si}~~ h_{si} [m], d) surface water speed v_{w} [$\mathrm{m\,s^{-1}}$], e) sea ice drift speed v_{si} [$\mathrm{m\,s^{-1}}$], f) 10m wind speed v_{a} [$\mathrm{m\,s^{-1}}$]. Time series of iceberg deterioration during the drift with g) iceberg mass loss per time step [$\mathrm{kg\,2h^{-1}}$] and contribution δ [$\mathrm{kg\,2h^{-1}}$] by h) wave erosion M_{e} , i) basal melt M_{fw} and j) buoyant convection M_{v}.

~~(Continuation of Fig. 9~~

Table 5. Statistics of ~~sea ice~~ environmental conditions along the of the trajectory of *iceberg 2013-788* with relative number of days in conditions with $CI > 15\%$, average sea ice concentration (CI), thickness (~~h_{si}~~h_{si}), sea surface temperature (SST), and total speed of 10m wind v_{a}, sea water surface v_{w} and sea ice ~~speed~~ v_{si}, along the trajectory. The sea ice speed is averaged over time periods with ~~relevant~~ sea ice ($CI > 15\%$).

	$\%\ CI > 15\%$	$\varnothing CI$ [%]	~~$\varnothing h_{si}$~~ $\varnothing h_{\mathrm{si}}$ [m]	$\varnothing SST$ [°C]	~~$\varnothing v_{ai}$~~ $\varnothing v_{\mathrm{si}}$ [m s−1]	~~$\varnothing v_w$~~ $\varnothing v_{\mathrm{w}}$ [m s−1]	~~$\varnothing v_a$~~ $\varnothing v_{\mathrm{a}}$ [m s−1]
Topaz	70	64	0.32	-1.27	0.05	0.13	6.95
Barents-2.5	77	74	0.42	-1.26	0.06	0.16	7.32
Topaz- Barents2.5	-7	-10	-0.1	+0.01	-0.01	-0.03	-0.37

Table 6. Difference of mean ~~absolute~~ total $2-$hourly deterioration rate (δ, 10^4 kg $2\mathrm{h}^{-1}$) and relative contributions by the deterioration terms (~~$\delta(term), \%$~~$\delta(M), \%$) in the ~~differently forced~~ trajectories of iceberg 2013-788 with different environmental input. The deterioration terms are melt erosion M_{e}, basal melt M_{fw} and buoyant vertical convection M_{v}

	δ	~~$\delta(M_e)$ %~~$\delta(M_{\mathrm{e}})$	~~$\delta(M_f w)$ %~~$\delta(M_{\mathrm{fw}})$	~~$\delta(M_v)$ %~~$\delta(M_{\mathrm{v}})$
Topaz-Barents2.5	-0.9	+5 ~~/-5~~	-5 ~~/-2~~	~~-0.01/-0.2~~-0.03

~~The iceberg deterioration rate (individual terms and sum of terms) is small () during the drift within sea ice and basal melt dominates (Fig. 9, means not shown). When the icebergs start to drift outside of the sea ice, the deterioration rates increase () and the contribution by wave erosion dominates. The total contribution by wave erosion is larger in Topaz-forced trajectories () , compared to Barents-2.5 forcing. The opposite is true for the basal melt (). The combined deterioration rate of *iceberg 2013-788* is in average smaller in Barents-2.5-forced trajectories (Table 6).~~

~~We highlight the period between 1 April and 15 May 2014, when the differently forced icebergs drift out of the relevant sea ice , to the east of Svalbard (Topaz-forced trajectories) and in the Central Basin (~~

5 Discussion

We investigate the impact of varied ocean, sea ice, and atmospheric input from four selected reanalyses, hindcasts and forecasts on the results of iceberg drift and deterioration simulations. We found that the environmental input causes a wide range of differences in the simulated iceberg characteristics.

5.1 Impact of environmental input on iceberg characteristics

Impact of ocean and sea ice variables on iceberg drift and deterioration

Ocean and sea ice variables have a large impact on the iceberg deterioration terms. Barents-2.5 ~~forced trajectories)~~yields larger values of CI ($+4\%$) and a longer exposure to sea ice in the iceberg pathways ($+23\%$). This reduces the deterioration due to

wave erosion in the iceberg simulations (−19%, Tab. 3). The impact of varied sea ice on iceberg deterioration is illustrated in the example of iceberg 2013-788 which shows smaller deterioration under Barents-2.5 input (Tab. 5, 6) and rapidly increasing deterioration terms when the icebergs drift out of the sea ice edge in April and May 2014 (~~Fig. 7). The general environmental situation in April 2013 can be described by the yearly maximum sea ice extent and infusions of warm Atlantic waters towards the sea ice edge (e.g. along the Hopen Trench and Central Basin) (Fig. 8) . Along the trajectories, the icebergs face decreasing sea ice concentration and thickness and increasing SST during their southward drift (~~Fig. 9). ~~The icebergs also face rapid changes in wind and water speed.~~

6 ~~Discussion~~

5.1 ~~Availability of forcing data~~

~~The availability of forcing data influences the simulation results of iceberg~~ This illustrates how the sensitivity of iceberg simulations to sea ice input is driven by the large impact on drift and deterioration~~(Bigg et al., 1997; Kubat et al., 2005; Eik, 2009b) . Simulations of iceberg drift and deterioration require forcing variables at a given time and position (Sect. 2.3). The availability of gridded forcing variables at this time and position depends on the general availability of the forcing dataset, the forcing data resolution, land-sea-mask, and the iceberg model setup (Herrmannsdörfer et al., 2024). Herrmannsdörfer et al. (2024) indicates, that the horizontal resolution and the land-sea-mask of the forcing data may be deciding factors for the forcing availability, when icebergs drift close to the coastline. The individual forcing datasets have different bathymetry and coastlines due to their horizontal resolution and grid orientation (rotation relative to latitude-longitude-grid) and type (e.g. curvilinear, regular).~~

~~The results of this study confirmed a dependency on the input data sets' horizontal resolution, bathymetry and land-sea-mask. Independent of the forcing dataset and its resolution, the majority of simulated trajectories and time steps have forcing available in the nearest grid cell, and a small minority lack forcing entirely. However, we found that the availability of forcing variables in the nearest grid cell varied with forcing data resolution and land-sea-mask. This small differences matter as they may cause large impact on the iceberg simulations.~~

~~We found a dependency on the horizontal forcing resolution and the search radius. In detail, the maximum search radius (in)within which forcing is available, is smaller for forcing with higher resolution. In addition, high-resolution forcing data allows for small step-wise increase in search radius (acting like a step-wise decrease of resolution). In this example , about $5 \cdot 5$ grid cells ($5 \cdot 2.5\,\mathrm{km}$) of the~~ , as well as the extensive occurrence of sea ice in the iceberg pathways. The average lower SST in Barents-2.5 ~~dataset equal one Topaz cell (of about $12.4 \cdot 12.4\mathrm{km}$). Thus, forcing from~~ ($-0.41\,^{\circ}\mathrm{C}$) in the iceberg pathways due to coupling with excessive sea ice (Sect. 3) decreases the deterioration for all terms (Tab. 3). This finding agrees with the previously found anti-correlation between SST and iceberg age in Keghouche et al. (2010). Larger water velocities in Barents-2.5 ~~is gathered at a higher resolution than variables from Topaz, even when not available in the nearest forcing cell, and resolution is decreased at a smaller rate. Comparing ERA5 and CARRA, ERA5's coarse resolution, especially in latitudinal direction (due to the regular grid), causes larger search radii. The impact of low horizontal resolution is largest in regions with~~

complex topography and bathymetry.($+0.05\,\mathrm{ms}^{-1}$) may explain larger basal melt, despite larger average Topaz SST (Sect. 3 and Tab. 3), which is also illustrated in the example of iceberg 2013-788 (Tab. 6). As a result, the total deterioration is smaller in simulations with Barents-2.5 input and favours longer drift duration and drift distance along the trajectory. Our findings also agree with the previously described relative importance of the deterioration terms (El-Tahan et al., 1987; Eik, 2009a) and sensitivity to the variables contributing to the iceberg drift (Kubat et al., 2005; Eik, 2009b; Keghouche et al., 2009, 2010).

Further, we find, that availability of low resolution atmospheric variables along the coastlines can be compensated by a more relaxed land-ocean-mask. This was achieved by masking at grid cell- water surface, according to the supplied land-mask of CARRA and ERA5. However, depending on the coastal topography, a more relaxed land-ocean-mask may decrease the representativity of the atmospheric variable for the ocean part of the cell.Note that this cannot be applied for the ocean variables, as they are produced on a fixed land-sea-mask.

The presented data assimilation approach (Sect. **??**) and dependency of forcing data availability on the horizontal resolution are important for a (precise as possible) physical simulation of iceberg close to coastlines. However, both high and low resolution ***Impact of ocean and sea ice variables on iceberg extension***

The differences in deterioration rates, drift duration and distance also cause variations in how far icebergs drift seasonally. Thus, varied ocean and sea ice models exhibit large errors in proximity to the coast, such as accumulation of water and ice (Idžanović et al., 2024). As iceberg simulations bridge the gap that is input cause relatively large differences in the lack of a statistically relevant number of observations, the propagation of those inaccuracies into the iceberg simulation must be accepted, and iceberg simulations close to the coast must be seen in the light of these inaccuracies.

5.1 Iceberg drift and deterioration

The theoretical influence of ocean, sea ice and atmosphere forcing on the iceberg drift is contrasting. While larger wind and sea water surface velocities increase the iceberg velocity and drift distance, they also contribute to the erosional and basal melt, due to a rougher sea state and higher differential velocity between iceberg and the sea. Positive seasonal iceberg extension in autumn (August-September) and early winter (November-December) (Fig. 6). This is because the seasonal and interannual variability of iceberg extension is inherited from the temporal variability of environmental variables. Keghouche et al. (2010) discovered a correlation between iceberg extension, CI and SST contribute to all deterioration terms. In the presence of sea ice, SST are around $-1.8°C$, thus the melt is reduced by lower SST and modulated waves. In sea ice concentrations over () , icebergs drift (solely) with the sea ice , setting the drift velocity and direction. We found significant differences in and we find similar dynamic (CI) and thermodynamic (SST) effects on the iceberg extension. Sea ice reduces the deterioration rate of the icebergs and may decrease the iceberg drift and deterioration due to varied forcing.

Iceberg deterioration The relative importance of the deterioration terms along the main iceberg pathways in the Barents Sea reflects the findings from El-Tahan et al. (1987) and Eik (2009a) in general, with largest contribution by wave erosion. The sensitivity of iceberg deterioration on sea ice can be seen well for iceberg 2013-788 in April and May 2014, when the icebergs drift out of sea iceedge and all deterioration terms increase rapidly.

The differences in relative importance in simulations with varied ocean and sea ice forcing highlight the importance of occurring sea ice conditions. As such, iceberg deterioration by wave erosion is decreased in Barents-2.5-forced iceberg simulations by its more extensive sea ice . In detail, Barents-2.5 provides more simulation time steps and trajectories with sea ice and the sea ice concentration is higher in the presence of speed. Higher temperatures and melt rates outside the sea ice limit the spread in the domain. We also find that sea ice increases the iceberg extension in spring, when icebergs drift far south within the sea ice, as the melt rates within the sea ice are low and sea ice , in expands far south. After the sea ice retreats in summer, icebergs are exposed to higher deterioration rates, limiting the spread in the domain until the sea ice expands again. Therefore, the iceberg pathways (**?**). Decreased deterioration (for all terms) in iceberg simulations forced by onset of sea ice growth in autumn could be a deciding factor for the iceberg extension later in the year. This timing of freeze-up and melt differ in Topaz (too fast, see Xie et al. (2017); Xie and Bertino (2022)) and Barents-2.5 is caused by average lower SST in Barents-2.5 (for iceberg pathways and throughout most of the domain, **?**), due to coupling with excessive sea ice . Larger basal melt, may be explained by larger water velocities in Barents-2.5, despite larger average Topaz SST. As Barents-2.5 suffers from a excessive representation of (delayed compared to Topaz, see Sect. 3). Keghouche et al. (2010) found no correlation with sea ice , related too small SST and too large velocities, due to its model setup, the decreased deterioration may be unrealistic. As the relative contribution of buoyant vertical convection is small, the differences due to varied forcing are insignificant.

Iceberg drift duration and distanceDecreased deterioration rates of thickness, however, we found that the exposure of iceberg to heavy sea ice and thus drift speed varies considerably between Topaz and Barents-2.5 -forced icebergs also favour longer drift duration and drift distance (along the trajectory). Drift duration and Track distance may be further increased by iceberg *looping*, due to tidal forcing.(Fig. 2, Tab. 2). Seasonal differences in wind speed and direction might contribute as well.

Slightly larger effective drift distances in Topaz-forced simulations might indicate, that including tidal components and local representation of variables might not alter how far the icebergs drift effectively. One might conclude that the tidal component is not essential to iceberg statistics in the Barents Sea, however we found that it is essential to simulating individual iceberg trajectories, iceberg occurrence (density) and extent in The iceberg extension is also influenced by the exact seeding, with size, position and seeding date, which varies within defined parameters in the statistics of this study and varies in other studies. In this study, the seasonal cycle is steered by iceberg seeding between July and November, so that lowest iceberg extension occurs just before the start of seeding in July and the larger extent occurs just after the end of the domainseeding, in late November. Seasonal seeding likely causes the difference to the seasonal cycle of iceberg extension in Keghouche et al. (2010) with maximum extension in June-July and minimum in October to November. The impact of the seeding seasonality on the iceberg extension is larger than the impact of the environmental input.

Small differences in iceberg ***Impact of ocean and sea ice variables on iceberg density***

The differences in deterioration rates, drift duration and distance between ERA5 and CARRA-forced simulations, are dominated by the differences in ocean and sea ice forcing.

ultimately also cause large spatial differences in spatial iceberg density, for example, around Svalbard and Franz-Josef-Land in Fig. 5. Differences in iceberg drift with varied forcing can be derived from different representation of these environmental regimes. As the differences from varied forcing are smaller than than the ones from different regions, we assume that the different forcing data sets could represent the differences between the regionally varying environmental regimes (e.g. different SST and CI). This may also be seen e.g. in similar main pathways from spatial densities and spatial extent.

5.1 Icebergs in the domain

We found that iceberg distribution and spread in the domain is dependent on the environmental forcing of ocean, sea ice and atmosphere. Spatial density differences may indicate an impact on the simulated iceberg pathways and large regional differences.

Iceberg density We found similar main pathways for all differently forced simulations. Iceberg density with varied input are as large as the absolute density and thus highly relevant. In general, iceberg density is largest in proximity to the iceberg sources (as in Keghouche et al. (2010)), as the average effective drift distance is only around 100 km (Sect. **??**4.1). The density is especially large when icebergs drift (loop) in the same regions for a long time. This is the case for Barents-2.5-forced trajectories, as they life longer due to decreased deterioration rates (Sect. **??**). As a consequence, average domain and local peak iceberg densities are higher for Barents-2.5-forced simulations.

Varied ocean- and sea ice-forcing cause large regional differences in iceberg density around Svalbard and Franz-Josef-Land. Differences of iceberg density due to varied forcing are as large as the absolute density and thus highly relevant. general distribution of the icebergs within the domain agrees with the findings of previous studies (e.g. Keghouche et al. (2010); Monteban et al. (20). The iceberg density is larger for Topaz-forced simulations simulations with Topaz input close to the coastlines and larger for simulations with Barents-2.5 -forced simulations in slightly larger input at slightly greater distance to the coastlines. This may be due to larger higher Barents-2.5 water speeds along the coastlines and slightly larger Topaz water speeds on the open ocean (**?**). It may also be due to different bathymetry, representation of the coastlines and horizontal resolution in the forcing data sets, that can alter the simulated density by iceberg grounding and the need for neighbour averaging, as described in Sect. 2.3. However, the (Sect. 3) that transport the icebergs towards the open oceans more quickly. The simulation results along the coastlines need to be viewed in the light of low viability of the forcing reliability of the environmental data in coastal regions.

Examples of the influence of the ocean and sea ice forcing on the iceberg densities are explained in the following. Higher iceberg densities in simulations with Barents-2.5 -forced simulations input in the northernmost parts of the domain may be explained by the forcing's Barents-2.5's average lower SST and thicker sea ice , that , higher concentration and more frequent (heavy) sea ice (Fig. 2), which increases the iceberg lifetime and may also trap traps the iceberg in those regions(**?**). Iceberg density differences around northern Novaya Zemlya may be related to large differences in surface water speed and direction and more frequent thick sea ice in the Barents-2.5 forcing (**?**) that prohibit a north- and westward drift. Large density differences north , as mentioned earlier by Keghouche et al. (2010).

Larger density to the north-west (north-east) of Bjørnøya ~~may evolve from lager forcing~~ under Topaz (Barents-2.5) input may result from large input differences in SST, water velocity and sea ice around the bathymetric feature of ~~the~~ Storfjorden Trough, Spitsbergen Bank and Hopen Trench ~~(?).~~ (Sect. 3). In contrast to Topaz, Barents-2.5 has complex spatial and temporal differences in water speed and direction, as it represents more local processes, including a strong tidal component and ~~complex water motion due to the complex bathymetry around the~~ topographically-steered currents around Spitsbergen Bank. ~~For more , the more~~ The more extensive sea ice cover over the Spitsbergen Bank in Barents-2.5, ~~might increase the release into open waters of~~ and the resulting reduced melt rate by wave erosion increases the number of icebergs drifting as far south as Hopen Trench.

~~Varied atmospheric forcing causes large differences in iceberg density on small spatial scales. This may be due to the resolution difference of the forcing datasets, that cause larger CARRA wind speeds in coastal areas and provide (more accurate)forcing between the islands of the~~ ***Effect of tides on iceberg characteristics***

The ocean input by Barents-2.5 further increases the drift duration, distance (Track) (Sect. 4.1), and local iceberg density (Sect. 4.2) by iceberg *looping*, as it prevents the icebergs from drifting directly into warmer waters, prolongs the track length and the time spent in a region. As a consequence, average domain and local peak iceberg densities are higher for simulations with Barents-2.5 input (Sect. 4.2). However, ocean input showed little impact on the effective drift distances. One might conclude that the tidal component is not essential to how far icebergs drift effectively in the Barents Sea (effective drift distance and extent, Fig. 3 and 4), however, we found that it is essential for simulating individual iceberg trajectories (Sect. 4.4), how long icebergs drift (drift duration, Fig. 3) and how many icebergs drift in different regions of the domain (regional iceberg density, Fig. 5).

Iceberg 2013-788 is influenced by tides, due to the oscillation of sea water speed along the trajectory (Fig. 9), but tidal forcing is too small in this example to be seen in Fig. 7. A relatively small influence by the tides may also explain characteristics of iceberg 2013-788 that contradict the above described statistics (longer drift duration and track for icebergs with Topaz input and longer effective distance for trajectories with Barents-2.5 input). Other iceberg trajectories in the simulations of this study showed examples with visible tidal looping, mostly in shallow regions where the tidal velocity is largest (e.g. Spitsbergen Bank).

Impact of atmospheric variables on iceberg characteristics

Wind input causes significant differences in iceberg density on small spatial scales. Higher horizontal resolution may cause higher wind speeds and (more accurate) atmospheric input between the islands of the Svalbard and Franz-Josef-Land ~~archipelago and in their fjords. Even though, the availability of forcing is assured close to the coast independent of the resolution (Sec. 2.3 and ??), the representability in complex topography is larger for higher resolution wind.High resolution ocean and sea ice forcing further increases the differences of varying the atmospheric forcing, as it allows the iceberg to drift closer to the coast. The deviation~~ archipelago, along their coastlines and in their fjords. The deviations of ERA5 and CARRA over sea ice ~~(?)~~

(Sect. 3) are compensated by the ~~decreased~~ low sensitivity of the iceberg drift to wind ~~forcing. The iceberg density is not impacted by atmospheric forcing on large scales.~~

input (within sea ice). In some regions varied ocean, sea ice, and ~~atmospheric-forcing~~ atmospheric input add up or cancel each other out, however the impact of varied ocean and sea ice ~~forcing is larger.Note, that because of the high resolution of Barents-2.5 and CARRA, icebergs can be forced to drift between islands and into fjords. Note that apparent iceberg occurrences on land are due to accumulating occurrences by a nearest neighbour method on an artificial grid of horizontal resolution (Sec. 2.3,4.2)~~ input generally dominates. The iceberg density is not impacted by atmospheric input on large scales.

~~***Iceberg extent***~~The example of iceberg 2013-788 illustrates the impact of environmental model physics, here wind representation over sea ice present in November 2013 to April 2014, (Fig. 9). The results are trajectories with small impact of wind input on large spatial scales, but visible impact on smaller spatial and temporal scales.

~~We found that iceberg extentvaries spatially and temporally~~

Wind input impacts seasonal iceberg extension on the same scale as varied ocean and sea ice input. Wind connected to large scale atmospheric patterns may also have an (delayed) impact on the interannual iceberg extension, as described in Keghouche et al. (2010).

Atmospheric input has no relevant impact on the drift distance (track, effective) or the spatial extent. The minor impact of atmospheric input may be explained by high similarity of ERA5 and CARRA wind over open ocean, due to ~~varied environmental forcing. Iceberg spread further in the domain (and in all directions)when forced by Barents-2.5. Especially the southward drift of icebergs is limited by the spatial distribution of *SST* and sea ice parameters, that are steered by large scale atmospheric patterns, global ocean currents and~~ the ~~bathymetry. Despite the existing deviations between the forcing data sets, iceberg drifted far south (to approximately), independent on the forcing~~extensive use of ERA5 in CARRA ((Hersbach et al., 2020; Køltzow et al., 2022), Sect. 3). Due to the high similarity wind input varies more with the trajectories of different ocean input, than between ERA5 and CARRA in the example of iceberg 2013-788 (Fig. 9).

~~The multi-year variability of iceberg extension is inherited from the environmental forcing. Beside environmental parameters with little multi-year variability (e.g. surface ocean velocity), sea ice conditions and wind can vary strongly. However, the multi-year variability of iceberg extension is also influenced by the exact seeding, with size, position and seeding date, which varies within defined parameters every year. The multi-year variability is largely reproduced by varied forcing.~~***Diverging trajectories and impact of resolution***

The example of iceberg 2013-788 demonstrates how identical initial conditions and small differences in the environmental input can result in diverging trajectories (causing increasing difference in input). This is due to the known tendency of Lagrangian trajectories to diverge and due to differences in environmental input, that induce differences in trajectory and further input differences. (Keghouche et al., 2009) described a rapid increase in the error in the iceberg simulation after two months.

~~The seasonal iceberg extension is influenced by the environmental conditions, especially by the seasonal cycle of SST and sea ice extent. Sea ice decreases the deterioration rate of the icebergs and may alter the iceberg drift speed, depending on the drift region. Larger temperatures and melt rates outside the sea ice limit the spread~~ The large impact by small environmental input differences can also be seen in the time period between 1 April and 15 May, when the iceberg 2013-788 drifts out of the sea ice and into regions with different ocean regimes (Fig. 9, 8). There, small change in iceberg position and different drift timing cause large difference in the exposure to environmental conditions and thereby iceberg drift and deterioration. This is also the case for coastal areas. It highlights the importance of temporal and horizontal resolution of the environmental data. An improvement in ocean and sea ice models would lead to extensive improvements in the iceberg simulations. In association, we observed that the high resolution of Barents-2.5 and CARRA allows icebergs to drift between islands and into fjords.

Impact of environmental input vs. regional and temporal variability

The difference in the simulation results (e.g. iceberg deterioration, drift duration, distance and seasonal iceberg extension, seen for the different iceberg sources in Fig. 3 and seasonal seeding in Fig. 6) due to varied environmental input are smaller than the spatial and temporal variability of the environmental variables in the domain. ~~Sea ice increases the iceberg extension in spring, when icebergs drift far south within the sea ice, as the melt rates within the sea ice are small and~~ The spatial variability of iceberg characteristics with the environmental input differences (e.g. SST difference in Barents-2.5 and Topaz) are dominated by the spatial differences in environmental regimes (e.g. iceberg size and regional sea ice characteristics). For example, icebergs from Franz-Josef-Land are larger, more frequently locked in sea ice ~~expands far south. After the sea ice retreat in summer, icebergs are exposed to largerdeterioration rates, limiting the spread in the domain until the sea ice expands again. Thereby, the onset of sea ice growth in the autumn could be a deciding factor for the iceberg extension later in the year. Seasonal differences in wind speed and direction might contributes as well.~~

~~The~~ due to the more extensive sea ice around Franz-Josef-Land, causing larger drift durations and spread in the domain (see also Keghouche et al. (2010)) compared to smaller icebergs from Novaya Zemlya that drift in mostly open waters. The temporal variability of iceberg characteristics (e.g. temporal iceberg extension) with the environmental input differences (e.g. in CI) is dominated by the seasonal and interannual variability of the environmental variables (e.g. the seasonal cycle of ~~iceberg extent in the Barents Sea sea is reproduced in all differently forced simulations, however with deviations. The variation of iceberg extension with environmental forcing can be seen in the relatively large differences in iceberg extension with varied~~ CI). This also means that the different environmental datasets distinguish the regionally and temporally varying environmental regimes well (in e.g. SST and CI). A similar representation of the environmental regimes may lead to similar main iceberg pathways.

Similarities in the iceberg characteristics despite varied environmental input

Despite the large impact of ocean and sea ice ~~forcing in autumn (August-September) and early winter (November-December)(Fig. 6) , that cannot be attributed to the seeding mechanism. Differences with atmospheric forcing are present from December to June.~~ input on iceberg drift and deterioration, and local impact of wind input described above, we found similar main pathways,

maximum spatial iceberg extent and southernmost latitude to where icebergs drifted (approximately 72°N). This may result from a similar general representation of the regional differences (e.g. between Central Bank and Spitsbergen Bank) in Topaz and Barents-2.5. One might conclude that the environmental input is not essential for simulating the main pathways and that these pathways are comparable in various studies.

5.1 Recommendations for practical applications

In the following, we discuss the suitability, advantages and disadvantages of the environmental model data (e.g. temporal availability and resolution of environmental data) as input in exemplary applications of iceberg simulations (e.g. long term statistics or short-time forecast of individual trajectories). This approach intends to support an informed decision on environmental input for iceberg simulations in future studies. We thereby outline which specific characteristics of an individual model (e.g. tides in Barents-2.5) causes which impact on iceberg simulations (e.g. spatial distribution). Note that we cannot provide generalised practical recommendations on which environmental data performs best as input to iceberg simulations, as the suitability is highly sensitive to the simulation goal, region, time period and model characteristics such as temporal and spatial availability, uncertainties, storage space and ease of access. The general lack of iceberg observations in the Barents Sea makes validating the statistics difficult.

~~The seasonal cycle of iceberg extension is also partly due to the seeding mechanisms and partly due to environmental conditions. The seasonal cycle is steered by iceberg seeding between July and November, so that lowest iceberg extension occurs just before the start of seeding in July and the larger extent occurs just after the end of the seeding, in late November. The influence of seeding mechanism on the results must be accounted for in the analysis.~~

5.2 ~~Example~~

~~The sensitivity of iceberg simulations~~ ***Long-term statistic applications, input availability, and comparability of studies***

Based on the above analysis, applications, including long-term statistics of iceberg pathways and the southernmost spatial iceberg extent (e.g. for analysing the long-term exposure of structures in the Central Barents Sea) are not sensitive to their environmental ~~forcing is illustrated by the example of *iceberg 2013-788*. The example demonstrates how small deviations in the environmental forcing lead to large deviations in the drift trajectory (and further deviation in forcing)~~ input. However, they are influenced by the availability of the input data (Bigg et al., 1997; Kubat et al., 2005; Eik, 2009b) and likely benefit from a wide time availability and consistency (e.g. in Topaz, ERA5 and CARRA). This study is strongly limited temporally and spatially due to the low availability of Barents-2.5.~~This can be seen by diverging trajectories of iceberg 2013-788 under varied ocean and sea ice forcing, despite similar initial conditions . The varied forcing ultimately leads to a different drift duration, drift into different regions, and differently far south, in the Barents Sea. Thus, the varied forcing also causes different potential exposure of structures and ships to icebergs.~~

The independence of the main iceberg pathways from the environmental input and the general similarity between the studies (e.g. in distribution of icebergs in the domain (Fig. 4) makes statistical iceberg studies comparable. Thus, the findings of this study are projectable on other studies, if accounting for the impact of different climatic conditions and different seeding conditions. We highlight that we do not study absolute iceberg characteristics as previous studies, but their differences due to varied environmental input. We highlight the novelty of this study, quantifying the impact of different types of common environmental models in iceberg simulations.

~~The large impact by small changes in the forcing can also be seen by in~~ ***Application of regional iceberg density simulations***

In applications simulating regional iceberg density (e.g. for planning of shipping routes around Spitsbergen Bank), the choice of input data is highly relevant. Differences in iceberg density are caused by different representation of ocean velocities, water temperature and sea ice, as e.g. found between Topaz and Barents-2.5 (Sect. 3) in the region around Bjørnøya. The region is characterised by warm Atlantic water inflow in the deeper parts (Storfjorden Trough and Hopen Trench), and southward cold-water transport in the shallower areas (Spitsbergen Bank), steering the water temperature and limiting the sea ice extent.

There, the ~~time period between 1 April and 15 May, when the iceberg drifts out of the sea ice and into regions with different ocean regimes. There, large changes in the iceberg drift and deterioration are caused by changing environmental forcing (of the same input data set) by small change in iceberg position and different timing. This also highlights the importance of temporal and horizontal resolution of the forcing data. The used forcing data sets showed large regional differences. The use of~~ topographically-steered currents and strong tidal influence in the shallow areas are described more extensively in Barents-2.5 (Fritzner et al., 2019; Röhrs et al., 2023; Idžanović et al., 2023, 2024). Topaz shows lower velocities, smaller gradients, and issues with simulating the circulation of Atlantic water inflow and the topographic steering (Sect. 3, REF). The sea surface velocity must be treated with special care, as the general lack of observations, limits the predictive skill of its forecasts and limits the constriction to observations in reanalyses. Despite the resulting low predictive skills in water velocities in both models, Barents-2.5 may ~~be beneficial due to its high horizontal~~ still benefit from the representation of tides, the effect of air pressure on the water surface, and high spatial and temporal resolution, compared to Topaz (Röhrs et al., 2023).

~~The large sensitivity to sea ice forcing can be seen in the large difference in iceberg drift forcing and deterioration upon ejection from the sea ice in spring 2014. It can also be seen by varied forcing causing a variation of exposure to sea ice in autumn, days within sea ice , which in this case causes less days with large deterioration and allows for a drift further south. The sensitivity to sea ice may also derive from its large presence along the iceberg pathways~~Sea ice and SST show large differences and uncertainties in Topaz and Barents-2.5 along the inflow of warm Atlantic waters and the spring sea ice edge (Sect. 3, Xie et al. (2017); Xie and Bertino (2022); Röhrs et al. (2023); Idžanović et al. (2024)). Overall, the decreased deterioration and elongated drift with Barents-2.5 input may be unrealistic due to its excessive representation of sea ice and too small SST known in the community. Despite the large uncertainties, Topaz's SST and sea ice variables are closer to observations which may allow for more realistic iceberg deterioration and therefore potentially also more realistic extent and

density. This applies especially for the year of 2010 to 2014, as the Barents-2.5 hindcast is a free-run, which tends to drift off, due to its missing constriction to input after the start of the model run (Idžanovic, pers. communications, 2024). Due to the large impact of sea ice representation on the iceberg simulations, it is therefore critical how well input data captures regional environmental regimes. Due to the large impact of sea ice concentration, iceberg simulations may benefit from using satellite-based CI products, although these are the basis for most of the sea ice models (e.g. Topaz, Barents-2.5 Forecast).

~~The minor impact of atmospheric forcing is shown by the smaller regional deviations of trajectories of iceberg 2013-788 with varied~~ Due to the local impact of wind input on iceberg density, we recommend considering also the choice of atmospheric input.~~It must be noted, that the *iceberg 2013-788* is initialised far north with above average size, causing a longer (and further south)drift than the average from the statistics of all $4 \cdot 7 \cdot 2603$ simulated icebergs. As such, the example is not suitable to explain the average differences of iceberg simulations with varied forcing, but serves as illustration of the forcing impact.~~

Application of individual iceberg trajectories

In the application of simulating individual trajectories of icebergs (e.g. to estimate the potential exposure of structures and ships), the choice of input data is highly relevant as drift and deterioration is dependent on all environmental variables (including wind), their spatial and temporal resolution and the tidal representation. Due to its high horizontal and temporal resolution, the use of Barents-2.5 may be beneficial in iceberg simulations, compared to the lower resolution Topaz data. We also recommend simulating an iceberg ensemble to account for uncertainties in the environmental input and initial conditions.

6 Conclusions

~~In~~ In the absence of sufficient iceberg observations in the Barents Sea, numerical simulations of iceberg drift and deterioration ~~are~~ serve as the most reliable source of data for iceberg statistics. We ~~found that the~~ simulated a large number of iceberg trajectories with varying environmental conditions in the Barents Sea and the years 2010-2014 and 2020-2021. We quantitatively confirm and novelly describe how the results of such simulations are sensitive to the input from ocean, sea ice and atmosphere reanalyses or forecasts. ~~The study exhibited both small forcing differences leading to large differences in iceberg trajectories and surprising similarities in the statistics, despite large forcing differences.~~

~~Large differences in the assimilated forcing information are caused by spatial and temporal resolution. Their horizontal resolution, bathymetry and coastline influence the availability of forcing information in the data assimilation into the iceberg model, distance of acquisition, representability of forcing information for the iceberg position and ultimately, the iceberg distribution and extent in the domain. This is especially visible along the coastlines. We highlight the importance of the forcing resolution's impact in coastal regions, despite the unreliable forcing information in those regions, due to the lack of other (environmental and iceberg) information in this region~~To explain these results, we statistically compared the environmental models in light of existing model validations. The findings are intended to guide the selection of environmental input and the

critical analysis of iceberg model simulations.

~~We found dependencies of the~~ We found that the environmental input influences the iceberg simulations results depending on the simulation goals, temporal and spatial settings and the environmental model uncertainty and availability. The sea ice input is especially relevant for estimating the exposure of structures or (seasonal) ship routes in icy waters. Decreased iceberg ~~simulations on all forcing variables, however, largest influence is found for the ocean and sea ice variables. Atmospheric forcing showed minor impact for most aspect for iceberg trajectories and statistics.~~

~~Sea ice showed especially large influence on iceberg simulations, e.g. for the forcing along the iceberg trajectory and the iceberg deterioration. Sea ice decreases the iceberg~~ deterioration, ~~thereby increasing the length of the drift durationand trajectory. A longer drift and e.g. looping increase the iceberg density , affecting the distribution in the domain.~~

~~Although, the effective drift distance is not widely influenced by varied ocean and sea ice forcing, varied ocean and sea ice forcing showed large impact on the occurrence and spread in the domain. Thereby, regional difference in iceberg density due to varied forcing can be high. The dependency of the simulation results on the environmental input highlight the importance of choice in forcing for generating iceberg statistics in~~ longer drift duration, and altered iceberg density are caused by an average $-0.41\,^{\circ}\mathrm{C}$ lower SST, 4% higher sea ice concentration and 23% more extensive sea ice occurrence in the ~~Barents Sea, e.g. for estimating the exposure of structures and ships.~~

~~Similarities in iceberg simulation results despite large forcing differences may be due to multiple compensating effects by varied forcing. Examples are found in a similar southernmost extent despite large deviations in spatial SST, or similar seasonal cycle in~~ iceberg ~~extent despite deviations in~~ pathways in Barents-2.5, compared to to Topaz. The representation of the onset of ~~sea ice freeze-up and melt. Other similarities may derive from a similar representation of the years and regions in the forcing data sets, despite differences in other aspects of the data sets (e.g. multi-year variability of iceberg extent and similar characteristics for icebergs from the same source~~freeze- and melt-up in the sea ice models steers the annual and multi-annual spread of icebergs in the domain (iceberg extension). The simulations using Barents-2.5 may be unrealistic due to excessive sea ice in Barents-2.5 (especially in the Hindcast, 2010-2014) compared to input from Topaz that is closer to the observations, despite large uncertainties (e.g. in the marginal ice zone) and a delayed seasonal cycle. Decreased uncertainty in the ocean and sea ice model would lead to significant improvements in iceberg simulations. The iceberg drift and density are further enhanced by a $0.05\,\mathrm{ms}^{-1}$ larger water speeds, tides and topographically-steered currents in Barents-2.5 (e.g. around Storfjorden Trough). This detailed local representation in Barents-2.5 is likely beneficial for iceberg simulations (e.g. for individual iceberg trajectories in shallow waters) despite its generally low skill in water velocity. Wind shows little impact on most iceberg characteristics, but the choice of higher-resolution input (e.g. CARRA) may be considered for simulations of local iceberg density and individual iceberg trajectories. In applications simulating individual iceberg trajectories, high temporal and horizontal resolution of the environmental data is important, as even small differences in the environmental input can result in diverging trajectories (e.g. as seen in the exemplary of iceberg 2013-788). We ~~emphasise the general similarity in the main icebergpathways, despite varied forcing.~~ highlight the importance of the input resolution in coastal regions, despite its unreliability due to the lack of other (both environmental and iceberg) data. The difference in iceberg characteristics are

dominated by the regional and seasonal regimes, which are represented in both Topaz and Barents-2.5. This may be the reason for similar iceberg pathways and their southernmost extent independent of the environmental input.

We comment We highlight that the study is restricted to the years of 2010-2014 and 2020-2021, the Barents Sea , a selection of four environmental models and the specific setup of the iceberg model. , due to temporal and spatial availability of the input data and the study goals. We also emphasise that we cannot provide clear suggestions on the best choice of environmental data in iceberg simulations, due to the diverse characteristics of the input data and the multifaceted impact on the simulations. However, the findings may be projectable on the other settings . widely agree with previous findings, are projectable on other settings and will facilitate the informed choice in environmental data. Future studies will concern themselves with conducting similar studies for a larger number of years, different regions (e.g. west Greenland) and assessing the performance of the iceberg simulations (under varied input) by comparing to iceberg drift observations.

Data availability. Data from ERA5 and CARRA are retrieved from the Copernicus Climate Data Store (Hersbach et al., 2023; Schyberg et al.). The Arctic Ocean Physics Renanalysis (Topaz) is available in Copernicus Marine (Xie, J., et al., 2017). The Barents-2.5 forecast and hindcast are stored by MET Norway (MET-Norway, a, c). Geostrophic currents are adopted from Slagstad et al. (1990) and bathymetry is gathered from Jakobsson et al. (2012).

Appendix A: Iceberg model and seeding

A1 Iceberg seeding

Main iceberg sources in the Barents Sea, respective seeding regions (blue) and number of seeded icebergs per simulations year (#).

2603 icebergs are initialised (*seeded*) with start date, position and length for every simulation year 2010-2014 and 2020-2021. The number of seeded icebergs refers to the satellite-based observations at the termini of the tidewater glaciers in the domain in Monteban et al. (2020). Start dates are drawn randomly at 00 UTC from 1 July to 30 November of the respective year. Start positions are drawn randomly from defined regions around the five main iceberg sources in the Barents Sea (see Fig. ??Fig. 1). Iceberg lengths are drawn randomly from a generalised extreme value distribution, described in Monteban et al. (2020).

$$f(x|k,\mu,\sigma) = \frac{1}{\sigma} exp(-(1+k\frac{x-\mu}{\sigma})^{-\frac{1}{k}})(1+k\frac{x-\mu}{\sigma})^{-1-\frac{1}{k}} \quad \text{(A1)}$$

Table A1. Parameters of the generalised extreme value distribution of iceberg length and average iceberg numbers at the main iceberg sources in the Barents Sea.

Source	Location μ	Scale σ	Shape k	Number N
Franz Josef Land West	44.963	14.156	0.402	351
Franz Josef Land East	46.480	15.636	0.252	542
Austfonna	44.501	10.668	0.118	909
Edgeøya	34.599	5.863	0.223	428
Novaya Zemlya	39.864	12.081	0.181	373

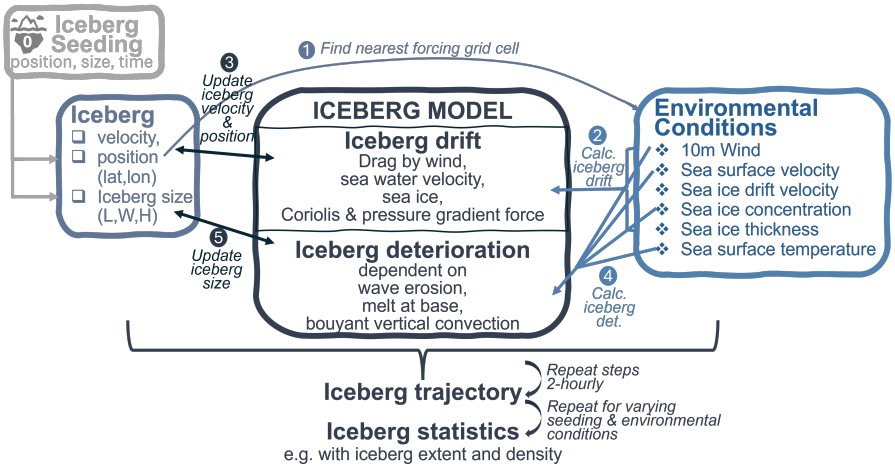

Figure A1. Schematic of iceberg model setup with iceberg seeding, drift and deterioration components, environmental ~~forcing~~input, and model output.

The distribution is fitted to satellite observations at the main sources, resulting in parameters in Table A1. With the given length L, width W and total height (sail plus keel) are calculated by the empirical relations in Dezecot and Eik (2015)

$$W = 0.7\,L\,exp(-0.000062\,L) \tag{A2}$$

$$H = 0.3\,L\,exp(-0.000062\,L) \tag{A3}$$

Seeding date, position and length are varied for different seeding years and sources, but is reproduced in the ~~differently forced simulations~~ simulations with different environmental input.

A2 Iceberg model setup and computational routine

The iceberg model components and computational routine are shown in Fig. A1. The iceberg is seeded, then ~~it's~~ its velocity $\boldsymbol{v}$ is updated for every $2-\text{hourly}$ time step dt by calculating the iceberg mass m and the iceberg acceleration $\frac{d\boldsymbol{v}}{dt}$ with the

equations of iceberg drift and the environmental input.

$$m = L \cdot W \cdot H \cdot \rho_i \cdot (1 - C_\mathrm{m}) \tag{A4}$$

$$\frac{d\boldsymbol{v}}{dt} = \frac{1}{m}[F_\mathrm{a} + F_\mathrm{w} + F_\mathrm{c,p} + F_\mathrm{si}] \tag{A5}$$

Afterwards, the iceberg dimensions L, W, H are updated with the equations of iceberg deterioration and the environmental input. The melt terms M are given in $\mathrm{ms}^{-}1$.

$$L = L + (-M_\mathrm{v} - M_\mathrm{e}) \cdot dt \tag{A6}$$

$$W = W + (-M_\mathrm{v} - M_\mathrm{e}) \cdot dt \tag{A7}$$

$$H = H + (-M_\mathrm{b}) \cdot dt \tag{A8}$$

The $2-\mathrm{hourly}$ updates are repeated until the iceberg is melted to the size of a growler ($\mathrm{H} \leq 10\,\mathrm{m}$), leaves the simulation domain or time period. in order to receive iceberg statistics, this approach is repeated for a large amount trajectories.

A3 Equations of iceberg drift

Iceberg drift can be expressed by physical iceberg mass m, added mass coefficient C_m, iceberg velocity $\boldsymbol{v}$, time t, Coriolis force F_c, pressure gradient force F_p, air and water form drag $F_\mathrm{a,w}$, wave radiation stress F_wd and sea ice forcing F_si (Savage, 2001).

$$m(1 + C_\mathrm{m})\frac{d\boldsymbol{v}}{dt} = F_\mathrm{c} + F_\mathrm{p} + F_\mathrm{a} + F_\mathrm{w} + F_\mathrm{wd} + F_\mathrm{si} \tag{A9}$$

Coriolis and pressure gradient force can be expressed as in Eq. A10, ~~where~~ in which the "Coriolis-related term" is calculated by subtracting the geostrophic velocity for geostrophic balance. Thereby, u, v and $u_\mathrm{geo}, v_\mathrm{geo}$ are the east- and northward components of the iceberg velocity vector $\boldsymbol{v}$ and geostrophic current velocity vector $\boldsymbol{v}_\mathrm{geo}$. Further variables are the Coriolis parameter $f = 2\Omega sin\phi$, Earth's rotation $\Omega = 2\pi\ \mathrm{day}^{-1}$, latitude ϕ and the vector normal to the Earth's surface $\boldsymbol{k}$. The geostrophic current is approximated with the ~~geostrophic current $u_\mathrm{geo}, v_\mathrm{geo}$ from Slagstad et al. (1990)~~ estimates in Slagstad et al. (1990)

$$F_\mathrm{c,p} = m \cdot f \cdot [v - v_\mathrm{geo}; -f - u - u_\mathrm{geo}] \tag{A10}$$

The form drag due to the surface water current and wind can be written as Eq. A11 and A12, with iceberg drift velocity $\boldsymbol{v}$, near surface water velocity $\boldsymbol{v}_\mathrm{w}$, $10\,m$ wind velocity $\boldsymbol{v}_\mathrm{a}$, water and air density $\rho_\mathrm{w,a}$ and water and air drag coefficient $C_\mathrm{w,a} \approx 1$. The cross section can be described by $A_\mathrm{w} = \frac{\rho_\mathrm{i}}{\rho_\mathrm{w}}\frac{2}{\pi}(L+W)H$ and $A_\mathrm{a} = \frac{\rho_\mathrm{w}-\rho_\mathrm{i}}{\rho_\mathrm{i}}A_\mathrm{w}$ with the iceberg dimensions length L, width W and the iceberg sail and keel height H. Density effects due to melting and dilution are neglected (Savage, 2001). The influence by the waves F_wd is modelled implicitly trough the wind drag coefficient (Monteban et al., 2020).

$$F_\mathrm{w} = \frac{1}{2}\rho_\mathrm{w} C_\mathrm{w} A_\mathrm{w} |(\boldsymbol{v}_\mathrm{w} - \boldsymbol{v})|(\boldsymbol{v}_\mathrm{w} - \boldsymbol{v}) \tag{A11}$$

$$F_\mathrm{a} = \frac{1}{2}\rho_\mathrm{a} C_\mathrm{a} A_\mathrm{a} |(\boldsymbol{v}_\mathrm{a} - \boldsymbol{v})|(\boldsymbol{v}_\mathrm{a} - \boldsymbol{v}) \tag{A12}$$

~~Sea ice influences the iceberg drift depending on sea ice velocity $\boldsymbol{v}_{\mathrm{si}}$, sea ice density ρ_{si}, drag coefficient C_{si} and cross section $A_{\mathrm{si}} = \frac{W+L}{2} h_{\mathrm{si}}$ (Savage, 2001). The high concentration case is applied under the condition that an ice thickness threshold $h_{\mathrm{si}} \geq h_{\mathrm{si,min}} = \frac{P}{P^* exp(-20(1-CI))}$ with $P = 13000$ and $P^* = 20000$ is fulfilled (Monteban et al., 2020).~~

$$F_{\mathrm{si}} = \begin{cases} 0 & \text{if } CI \leq 15\% \\ -(F_{\mathrm{c}} + F_{\mathrm{p}} + F_{\mathrm{a}} + F_{\mathrm{w}}) + \frac{d\boldsymbol{v}_{\mathrm{si}}}{dt} & \text{if } CI \geq 90\% \\ \frac{1}{2}\rho_{\mathrm{si}} C_{\mathrm{si}} A_{\mathrm{si}} |(\boldsymbol{v}_{\mathrm{si}} - \boldsymbol{v})|(\boldsymbol{v}_{\mathrm{si}} - \boldsymbol{v}) & \text{otherwise} \end{cases} \tag{A13}$$

A4 Equations of iceberg deterioration

Iceberg deterioration can be described by deterioration due to solar radiation M_{s}, buoyant vertical convection M_{v}, forced convection by air and water $M_{\mathrm{fw,fa}}$, wave erosion M_{e} and wave calving M_{cal} (Kubat et al., 2007; Eik, 2009a) (Eq. A14).

$$M_{\mathrm{total}} = M_{\mathrm{s}} + M_{\mathrm{v}} + M_{\mathrm{fa}} + M_{\mathrm{fw}} + M_{\mathrm{e}} + M_{\mathrm{cal}} \tag{A14}$$

The terms contribute to the total deterioration at different rates with highest impact from wave erosion (with calving), forced convection by water, and to a much smaller degree buoyant convection (El-Tahan et al., 1987; Savage, 2001; Kubat et al., 2007; Eik, 2009a). In this study, the effect of solar radiation and forced convection by wind is neglected. Due to its complexity, calving is not explicitly described. The erosional melt M_{e} due to waves is described by sea surface temperature SST, sea ice concentration CI and sea state $Ss = \frac{3}{2}|V_{\mathrm{a}} - V_{\mathrm{w}}|^{0.5} + 0.1|V_{\mathrm{a}} - V_{\mathrm{w}}|$ with total wind and current speed $V_{\mathrm{a,w}}$ (Eq. A15, (Gladstone et al., 2001)).

$$M_{\mathrm{e}} = \frac{(\frac{1}{6}[SST + 2])Ss(0.5[1 + cos(CI^3\pi)])}{24 \cdot 3600} \tag{A15}$$

The melt due to buoyant vertical convection M_{v} is given by the freezing point temperature $t_{\mathrm{fp}} = t_{\mathrm{fs}} \cdot exp(-0.19 \cdot [SST - t_{\mathrm{fs}}])$, sea water freezing temperature $t_{\mathrm{fs}} = -0.036 - 0.0499 \cdot Sal - 0.000112 \cdot (Sal^2)$ and Salinity $Sal = 34.8$ (Eq. A16).

$$M_{\mathrm{v}} = 8.8 \cdot 10^{-8}[SST - t_{\mathrm{fp}}] + 1.5 \cdot 10^{-8}[SST - t_{\mathrm{fp}}]^2 \tag{A16}$$

The forced convection by water M_{fw} or turbulent basal melt is calculated by the East/North component of the iceberg and water drift u, v and u_{w}, v_{w}, the iceberg length L and the ice temperature close to the water interface T_{i} of $-4°C$ (Eq. A17).

$$M_{\mathrm{fw}} = 6.7 \cdot 10^{-6} \sqrt{(u - u_{\mathrm{w}})^2 + (v - v_{\mathrm{w}})^2}^{0.8} \cdot (SST - T_{\mathrm{i}}) \cdot L^{-0.2} \tag{A17}$$

A5 ~~Model parameters~~

Table A2 and A3 show the parameters used in the iceberg simulations.

Author contributions. Data pre-processing, model adaptions, simulations, statistical analysis and original draft of manuscript: LH. Supervision during all stages of the study and review of the manuscript: RKL, KVH.

Table A2. Coefficients of iceberg drift and deterioration.

	Description	Value	Reference
C_{m}	Added mass coefficient	0	Keghouche et al. (2009); Monteban et al. (2020)
C_{w}	Water drag coefficient	0.25	Keghouche et al. (2009)
C_{a}	Air drag coefficient	0.7	Monteban et al. (2020)
C_{si}	Sea ice drag coefficient	1.0	Eik (2009b)

Table A3. Physical parameters of ocean, atmosphere and sea ice for the simulation of iceberg drift and deterioration.

	Description	Value	Reference
ρ_{w}	Water density	$1027\,\mathrm{kg\,m^{-3}}$	-
ρ_{a}	Air density	$1.225\,\mathrm{kg\,m^{-3}}$	-
ρ_{si}	Sea ice density	$900\,\mathrm{kg\,m^{-3}}$	-
ρ_{i}	Iceberg density	$850\,\mathrm{kg\,m^{-3}}$	Monteban et al. (2020)
T_{i}	Iceberg temperature	$-4^{\circ}\mathrm{C}$	Wagner et al. (2017)

Competing interests. The authors declare that they have no conflict of interest.

Acknowledgements. The authors wish to acknowledge the support from the Research Council of Norway through the RareIce project (326834) and the support from all RareIce partners. The authors also wish to acknowledge Dennis Monteban, for supporting the understanding of the iceberg model.

The ERA5 (Hersbach et al., 2023) and CARRA data (Schyberg et al.) were downloaded from the Copernicus Climate Change Service (2023). The results contain modified Copernicus Climate Change Service information 2023. Neither the European Commission nor ECMWF is responsible for any use that may be made of the Copernicus information or data it contains. This study has been conducted using E.U. Copernicus Marine Service Information, ~~(?)~~(Xie, J., et al., 2017).

References

Abramov, V. and Tunik, A.: Atlas of Arctic Icebergs: The Greenland, Barents, East- Siberian and Chukchi Seas in the Arctic Basin, Backbone Publ. Co., 1996.

Bigg, G. R., Wadley, M. R., Stevens, D. P., and Johnson, J. A.: Modelling the dynamics and thermodynamics of icebergs, Cold Regions Science and Technology, 26, 113–135, https://doi.org/10.1016/S0165-232X(97)00012-8, 1997.

Dezecot, C. and Eik, K.: Barents East blocks Metocean Design Basis, Statoil Report, document no.: ME2015-005, 2015.

Eik, K.: Iceberg deterioration in the Barents sea, Proceedings of the International Conference on Port and Ocean Engineering under Arctic Conditions, POAC, 2, 913–927, 2009a.

Eik, K.: Iceberg drift modelling and validation of applied metocean hindcast data, Cold Regions Science and Technology, 57, 67–90, https://doi.org/10.1016/j.coldregions.2009.02.009, 2009b.

El-Tahan, M., Venkatesh, S., and El-Tahan, H.: Validation and Quantitative Assessment of the Deterioration Mechanisms of Arctic Icebergs, Journal of Offshore Mechanics and Arctic Engineering, 109, 102–108, https://doi.org/10.1115/1.3256983, 1987.

Fritzner, S., Graversen, R., Christensen, K. H., Rostosky, P., and Wang, K.: Impact of assimilating sea ice concentration, sea ice thickness and snow depth in a coupled ocean–sea ice modelling system, The Cryosphere, 13, 491–509, https://doi.org/10.5194/tc-13-491-2019, 2019.

Giusti, M., et al.: Copernicus Arctic Regional Reanalysis (CARRA): Added value to the ERA5 global reanalysis., https://confluence.ecmwf.int/display/CKB/Copernicus+Arctic+Regional+Reanalysis+%28CARRA%29%3A+Added+value+to+the+ERA5+global+reanalysis, accessed 18 Apr 2024, 2024.

Gladstone, R. M., Bigg, G. R., and Nicholls, K. W.: Iceberg trajectory modeling and meltwater injection in the Southern Ocean, Journal of Geophysical Research: Oceans, 106, 19 903–19 915, https://doi.org/https://doi.org/10.1029/2000JC000347, 2001.

Herrmannsdörfer, L., Lubbad, R. K., and Høyland, K. V.: Requirements on environmental forcing for models of iceberg drift and deterioration in the Barents Sea, Proceedings of the 27th IAHR International Symposium on Ice, 2024.

Hersbach, H., Bell, B., Berrisford, P., Hirahara, S., Horányi, A., Muñoz-Sabater, J., Nicolas, J., Peubey, C., Radu, R., Schepers, D., Simmons, A., Soci, C., Abdalla, S., Abellan, X., Balsamo, G., Bechtold, P., Biavati, G., Bidlot, J., Bonavita, M., De Chiara, G., Dahlgren, P., Dee, D., Diamantakis, M., Dragani, R., Flemming, J., Forbes, R., Fuentes, M., Geer, A., Haimberger, L., Healy, S., Hogan, R. J., Hólm, E., Janisková, M., Keeley, S., Laloyaux, P., Lopez, P., Lupu, C., Radnoti, G., de Rosnay, P., Rozum, I., Vamborg, F., Villaume, S., and Thépaut, J.-N.: The ERA5 global reanalysis, Quarterly Journal of the Royal Meteorological Society, 146, 1999–2049, https://doi.org/https://doi.org/10.1002/qj.3803, 2020.

Hersbach, H., Bell, B., Berrisford, P., Biavati, G., Horányi, A., Muñoz Sabater, J., Nicolas, J., Peubey, C., Radu, R., Rozum, I., Schepers, D., Simmons, A., Soci, C., Dee, D., and Thépaut, J.-N.: ERA5 hourly data on single levels from 1940 to present, Copernicus Climate Change Service (C3S) Climate Data Store (CDS), https://doi.org/10.24381/cds.adbb2d47, (Accessed on 20 Aug 2023), 2023.

Idžanović, M., Rikardsen, E. S. U., and Röhrs, J.: Forecast uncertainty and ensemble spread in surface currents from a regional ocean model, Frontiers in Marine Science, 10, https://doi.org/10.3389/fmars.2023.1177337, 2023.

Idžanović, M., Rikardsen, E. S. U., Matuszak, M., Wang, C., and Trodahl, M.: Barents-2.5km: an ocean and sea ice hindcast for the Barents Sea and Svalbard (Report No. 13/2024), Norwegian Meteorological Institute, in progress, 2024.

Jakobsson, M., Mayer, L., Coakley, B., Dowdeswell, J. A., Forbes, S., Fridman, B., Hodnesdal, H., Noormets, R., Pedersen, R., Rebesco, M., Schenke, H. W., Zarayskaya, Y., Accettella, D., Armstrong, A., Anderson, R. M., Bienhoff, P., Camerlenghi, A., Church, I., Edwards, M., Gardner, J. V., Hall, J. K., Hell, B., Hestvik, O., Kristoffersen, Y., Marcussen, C., Mohammad, R., Mosher, D., Nghiem, S. V., Pedrosa,

M. T., Travaglini, P. G., and Weatherall, P.: The International Bathymetric Chart of the Arctic Ocean (IBCAO) Version 3.0, Geophysical Research Letters, 39, https://doi.org/doi.org/10.1029/2012GL052219, 2012.

Keghouche, I., Bertino, L., and Lisæter, K. A.: Parameterization of an Iceberg Drift Model in the Barents Sea, Journal of Atmospheric and Oceanic Technology, 26, 2216 – 2227, https://doi.org/10.1175/2009JTECHO678.1, 2009.

Keghouche, I., Counillon, F., and Bertino, L.: Modeling dynamics and thermodynamics of icebergs in the Barents Sea from 1987 to 2005, Journal of Geophysical Research: Oceans, 115, https://doi.org/10.1029/2010JC006165, 2010.

Kubat, I., Sayed, M., t, S. B., and Carrieres, T.: An Operational Model of Iceberg Drift, International Journal of Offshore and Polar Engineering, 15, 2005.

Kubat, I., Savage, S., Carrieres, T., and Crocker, G.: An Operational Iceberg Deterioration Model, Proceedings of the International Offshore and Polar Engineering Conference, 2007.

Køltzow, M., Casati, B., Bazile, E., Haiden, T., and Valkonen, T.: An NWP Model Intercomparison of Surface Weather Parameters in the European Arctic during the Year of Polar Prediction Special Observing Period Northern Hemisphere, Weather and Forecasting, 34, 959 – 983, https://doi.org/10.1175/WAF-D-19-0003.1, 2019.

Køltzow, M., Schyberg, H., Støylen, E., and Yang, X.: Value of the Copernicus Arctic Regional Reanalysis (CARRA) in representing near-surface temperature and wind speed in the north-east European Arctic, Polar Research, 41, https://doi.org/10.33265/polar.v41.8002, 2022.

MET-Norway: Barents-2.5 ocean and ice forecast archive (ROMS, Prodcution end 2022), Norwegian Meteorological Institute, https://thredds.met.no/thredds/fou-hi/barents25.html, (Accessed on 30-Aug-2023), a.

MET-Norway: Barents-2.5 ocean and ice forecast archive (ROMS-EPS), Norwegian Meteorological Institute, https://thredds.met.no/thredds/fou-hi/barents_eps.html, (Accessed on 30-Aug-2023), b.

MET-Norway: Barents-2.5 ocean and ice hindcast archive, Norwegian Meteorological Institute, https://thredds.met.no/thredds/catalog/romshindcast/barents2500_2010/catalog.html, (Accessed on 30-Aug-2023), c.

Monteban, D., Lubbad, R., Samardzija, I., and Løset, S.: Enhanced iceberg drift modelling in the Barents Sea with estimates of the release rates and size characteristics at the major glacial sources using Sentinel-1 and Sentinel-2, Cold Regions Science and Technology, 175, 103 084, https://doi.org/10.1016/j.coldregions.2020.103084, 2020.

Röhrs, J., Gusdal, Y., Rikardsen, E. S. U., Durán Moro, M., Brændshøi, J., Kristensen, N. M., Fritzner, S., Wang, K., Sperrevik, A. K., Idžanović, M., Lavergne, T., Debernard, J. B., and Christensen, K. H.: Barents-2.5km v2.0: an operational data-assimilative coupled ocean and sea ice ensemble prediction model for the Barents Sea and Svalbard, Geoscientific Model Development, 16, 5401–5426, https://doi.org/10.5194/gmd-16-5401-2023, 2023.

Röhrs, J., Sutherland, G., Jeans, G., Bedington, M., Sperrevik, A., Dagestad, K.-F., Gusdal, Y., Mauritzen, C., Dale, A., and LaCasce, J.: Surface currents in operational oceanography: Key applications, mechanisms, and methods, Journal of Operational Oceanography, 16, 60–88, https://doi.org/10.1080/1755876X.2021.1903221, 2023.

Sakov, P., Counillon, F., Bertino, L., Lisæter, K. A., Oke, P. R., and Korablev, A.: TOPAZ4: an ocean-sea ice data assimilation system for the North Atlantic and Arctic, Ocean Science, 8, 633–656, https://doi.org/10.5194/os-8-633-2012, 2012.

Savage, S.: Aspects of Iceberg Deterioration and Drift, pp. 279–318, Springer Berlin Heidelberg, Berlin, Heidelberg, ISBN 978-3-540-45670-4, https://doi.org/10.1007/3-540-45670-8_12, 2001.

Schyberg, H., Yang, X., Køltzow, M., Amstrup, B., Bakketun, A., Bazile, E., Bojarova, J., Box, J. E., Dahlgren, P., Hagelin, S., Homleid, M., Horányi, A., Høyer, J., Johansson, A., Killie, M., Körnich, H., Le Moigne, P., Lindskog, M., Manninen, T., Nielsen Englyst, P., Nielsen, K., Olsson, E., Palmason, B., Peralta Aros, C., Randriamampianina, R., Samuelsson, P., Stappers, R., Støylen, E., Thorsteinsson, S., Valkonen,

T., and Wang, Z. .: Arctic regional reanalysis on single levels from 1991 to present, Copernicus Climate Change Service (C3S) Climate Data Store (CDS), https://doi.org/10.24381/cds.713858f6, (Accessed on 22 Aug 2023).

Slagstad, D., Støle-Hansen, K., and Loeng, H.: Density driven currents in the Barents Sea calculated by a numerical model, Modeling, Identification and Control (MIC), 11, 181–190, https://doi.org/10.4173/mic.1990.4.1, 1990.

Wagner, T. J. W., Dell, R. W., and Eisenman, I.: An Analytical Model of Iceberg Drift, Journal of Physical Oceanography, 47, 1605 – 1616, https://doi.org/10.1175/JPO-D-16-0262.1, 2017.

Xie, J. and Bertino, L.: Quality infromation Document - Arctic Physical Multi Year Product ARCTIC_MULTIYEAR_PHY_002_003, Tech. rep., E.U. Copernicus Marine Service Information (CMEMS). Marine Data Store (MDS), https://doi.org/10.48670/moi-00007, 2022.

Xie, J., Bertino, L., Counillon, F., Lisæter, K. A., and Sakov, P.: Quality assessment of the TOPAZ4 reanalysis in the Arctic over the period 1991–2013, Ocean Science, 13, 123–144, https://doi.org/10.5194/os-13-123-2017, 2017.

Xie, J., et al.: Arctic Ocean Physics Reanalysis, E.U. Copernicus Marine Service Information (CMEMS). Marine Data Store (MDS), https://doi.org/10.48670/moi-00007, (Accessed on 03-Aug-2023), 2017.

Yang, X., Schyberg, H., Palmason, B., Bojarova, J., Pagh, N. K., Dahlborn, M., Peralta, C., Homleid, M., Køltzow, M., Randriamampianina, R., Dahlgren, P., Vignes, O., Støylen, E., Valkonen, T., Lindskog, M., Hagelin, S., Körnich, H., and Thorsteinsson, S.: Complete test and verification report on fully configured reanalysis and monitoring system, https://cds.climate.copernicus.eu/cdsapp#!/dataset/reanalysis-carra-single-levels, (accessed on 06-Jan-2023), 2020.